Journal of King Saud University - Computer and Information Sciences 36 (2024) 101940

HOSTED BY

Contents lists available at ScienceDirect

Journal of King Saud University - Computer and Information Sciences

journal homepage: www.sciencedirect.com

Full length article

Classification of Alzheimer's disease using MRI data based on Deep Learning Techniques

Shaymaa E. Sorour [a,b,*], Amr A. Abd El-Mageed [c], Khalied M. Albarrak [a], Abdulrahman K. Alnaim [a], Abeer A. Wafa [d], Engy El-Shafeiy [e]

[a] Department of Management Information Systems, College of Business Administration, King Faisal University, Al-Ahsa 31982, Saudi Arabia
[b] Faculty of Specific Education, Kafrelsheikh University, Kafrelsheikh, 33511, Egypt
[c] Department of Information Systems, Sohag University, Sohag, 82511, Egypt
[d] Faculty of Computers and Artificial Intelligence, Helwan University, Egypt
[e] Faculty of Computers and Artificial Intelligence, University of Sadat City, Sadat City, Menofia, Egypt

ARTICLE INFO

Keywords:
Alzheimer's disease (AD)
Magnetic resonance imaging (MRI)
Deep learning (DL)
CNNs-without-aug
CNNs-with-aug
CNNs-LSTM-with-aug
CNNs-SVM-with-aug
VGG16-SVM-with-aug

ABSTRACT

Alzheimer's Disease (AD) is a worldwide concern impacting millions of people, with no effective treatment known to date. Unlike cancer, which has seen improvement in preventing its progression, early detection remains critical in managing the burden of AD. This paper suggests a novel AD-DL approach for detecting early AD using Deep Learning (DL) Techniques. The dataset consists of pictures of brain magnetic resonance imaging (MRI) used to evaluate and validate the suggested model. The method includes stages for pre-processing, DL model training, and evaluation. Five DL models with autonomous feature extraction and binary classification are shown. The models are divided into two categories: without Data Augmentation (without-Aug), which includes CNN-without-AUG, and with Data Augmentation (with-Aug), which includes CNNs-with-Aug, CNNs-LSTM-with-Aug, CNNs-SVM-with-Aug, and Transfer learning using VGG16-SVM-with-Aug. The main goal is to build a model with the best detection accuracy, recall, precision, F1 score, training time, and testing time. The dataset is used to evaluate the recommended methodology, showing encouraging results. The experimental results show that CNN-LSTM is superior, with an accuracy percentage of 99.92%. The outcomes of this study lay the groundwork for future DL-based research in AD identification.

1. Introduction

AD accounts for 70% of dementia cases worldwide, making it the most prevalent kind of dementia. It is an irreversible neurological condition that gradually impairs cognitive ability. AD is a huge global concern that affects millions of people despite the lack of a proven treatment protocol. While treatment options for certain diseases, such as cancer, have advanced, early detection remains critical for adequately managing AD (Khojaste-Sarakhsi et al., 2022; Vogt et al., 2023; Saleem et al., 2022). According to research, AD is assumed to begin at least 20 years before symptoms manifest, with minute, subtle alterations in the brain. Because of injured or killed nerve cells (neurons) in specific brain regions, people will eventually exhibit observable symptoms such as memory loss and language difficulties after years of brain alterations. Usually, people with AD endure their symptoms for years. The severity of symptoms tends to worsen over time, impairing an individual's capacity to carry out daily tasks. As there is presently no known cure for AD, existing therapies concentrate on slowing the disease's progression to its most advanced state. To enhance patients' quality of life and more effectively handle the years in which they become incapable of making decisions (Farina et al., 2020; Odusami et al.,

* Corresponding author at: Department of Management Information Systems, College of Business Administration, King Faisal University, Al-Ahsa 31982, Saudi Arabia.
E-mail addresses: ssorour@kfu.edu.sa (S.E. Sorour), amr.atef@commerce.sohag.edu.eg (A.A.A. El-Mageed), kalbarrak@kfu.edu.sa (K.M. Albarrak), aalnaim@kfu.edu.sa (A.K. Alnaim), abeerabdelnasser9@gmail.com (A.A. Wafa), Engy.elshafeiy@gmail.com (E. El-Shafeiy).
Peer review under responsibility of King Saud University.

Production and hosting by Elsevier

https://doi.org/10.1016/j.jksuci.2024.101940
Received 5 November 2023; Received in revised form 5 January 2024; Accepted 20 January 2024
Available online 24 January 2024

2023; Ávila-Jiménez et al., 2023; Prasath and Sumathi, 2024). This research describes a unique DL-based technique for the early detection of AD. The study intends to test the approach's usefulness in diagnosing early-stage AD using brain MRI data. Individuals aged 65 and older are more vulnerable to AD in developed countries (Sosa-Ortiz et al., 2012; Fathi et al., 2022; Diogo et al., 2022).

According to projections, about 0.64 billion of people worldwide will be analyzed with AD between now and 2050. This condition not only offers substantial social and economic issues, as evidenced by the accompanying material, but it also has terrible consequences for those afflicted and their families, who carry the tremendous burden of providing care for the patient. There are several methodologies for establishing a diagnosis when considering computer-aided diagnosis systems. These procedures include various cognitive, neurological, and psychological examinations, as well as the minor mental state (MMS) assessment and the Modified minor mental evaluation. Several technical and biological exams can be performed in addition to these tests to boost the diagnostic procedure. Through lumbar puncture, for example, biomarkers in cerebrospinal fluid (CSF) can be identified, and various imaging modalities such as MRI, tractography (also known as Diffusion Tensor Imaging or DTI), and Positron Emission Tomography (PET) are utilized to supplement and enhance the detection of AD. Numerous strategies have been developed to use biomarkers in 3D MRI images to classify patients' current states and forecast the progression to AD (Leela et al., 2023). AD is diagnosed by brain monitoring techniques such as MRI, Computer Tomography (CT) scans, and PET. MRI is a powerful tool for detecting disease-related brain structure and function changes. It is regarded as a valuable and crucial tool for detecting early indicators of AD. MRI has several benefits because it does not require any surgical procedures and enables noninvasive and comprehensive brain imaging. Its high-resolution imaging capabilities, capacity to capture structural alterations in the brain, and role in monitoring disease progression make it an invaluable tool for clinicians, researchers, and patients (Lakhan et al., 2023).

In the last few years, Machine Learning (ML) and DL methods have been offered, adopted, and implemented for analyzing various pictures and MRIs. These algorithms have been especially beneficial in diagnosing health concerns and recognizing early indicators of AD. Furthermore, they have demonstrated extraordinary ability in picture identification and classification across a variety of sectors, including healthcare, computer vision, and others (Jindal et al., 2021; Saini and Marriwala, 2022; Nalini and Rama, 2022; Sharma and Guleria, 2022; Trivedi et al., 2022). There has been tremendous growth in neuroimaging data over the last few decades, greatly aiding in characterizing AD utilizing ML and DL approaches. Researchers have used similar approaches to obtain encouraging results in the individual AD diagnosis and forecast (Nagarajan et al., 2021). To analyze AD, multiple classifiers, like random forest, decision tree, and Support Vector Machine (SVM), have been applied to specified characteristics collected from image processing pipelines from diverse research. DL approaches have recently emerged as a significant advancement in the medical imaging field, delivering excellent picture categorization success rates (Ajagbe et al., 2021). DL methods that are often employed include Convolutional Neural Network (CNN), Artificial Neural Network (ANN), and Transfer Learning. Compared to ML, DL models enable automatic abstraction of picture characteristics from low to high levels, significantly facilitating feature representation (Raju et al., 2021).

Several DL methods, such as the SVM with particle swarm optimization (PSO) and CNN, have been extensively employed to forecast the phases of AD, displaying good performance and high accuracy (Saied et al., 2021). The shrinking phenomena reported in the Hippocampal area is the most thoroughly examined of these biomarkers. As a result, various methods for classifying MRI scans for population screening have been developed, emphasizing the hippocampus area and other indicators in the brain. In this investigation, the claim made was supported in Wang et al. (2020) that exact segmentation of the total brain volume is not required. Instead, a rough identification of the biomarker region is sufficient, achieved through brain alignment and atlas-based selection of the region-of-interest (ROI) (Wang et al., 2020). Following that, traditional multimedia indexing approaches can be used to the selected ROI by using feature-based visual signatures produced from "engineered features" or by deploying state-of-the-art CNNs that have successfully classified visual and multimedia data. DL approaches entail a stage-by-stage transformation and learning of input data, resulting in progressively complicated and abstract representations. The original pixel matrix is abstracted and edge-encoded in applications that use input images. Following that, the edges are organized and encoded, and other image features are composed, resulting in a representation of the input image (Nagarajan et al., 2022).

However, there are several difficulties in the area of damage identification. These involve the labeled data scarcity, the high complexity of DL models, and the preference for relatively shallow DL models for defect diagnosis, with above five hidden layers. On the other hand, CNN models developed for ImageNet classification tasks frequently have several layers. As CNN models for defect detection are generally shallow, their usefulness and last accuracy of defect diagnosis predictions may be limited. Training a sufficiently deep CNN model becomes difficult because of the scarcity of well-managed datasets similar to ImageNet. For addressing this problem, researchers used transfer learning in conjunction with CNN models. They first build a deep CNN model on the ImageNet dataset and then use the trained CNN model as a feature extractor on smaller datasets. This strategy has shown outstanding results (Biagetti et al., 2021). Furthermore, early or later developed fusion techniques must be adapted to address the classification problem of AD utilizing a single MRI (SMRI) modality (such as three different projections in SMRI) or multiple modalities, such as SMRI and DTI. The categorization performance was improved by doing so. Several pre-trained CNN models, including AlexNet, deepNN, ResNet-50, VGG11, ResNet-34, SqueezeNet, DenseNet, and InceptionV3, have outperformed others in automatically diagnosing the phases of AD using MRI scans (Odusami et al., 2022). These pre-trained models have been used successfully in MRI analysis and can capture critical structural information for identifying different stages of AD. This contrasts with a system that trains a single structure entirely on MRI data.

The significance of using DL in early AD detection is that it can accurately and precisely evaluate enormous amounts of medical imaging data. They can spot tiny AD-related patterns and biomarkers that would be hard to find using more conventional techniques. Early AD detection allows for timely therapy and intervention, reduces the disease trajectory, and successfully manages symptoms. Patients' and their families' quality of life could be significantly enhanced. DL models give objective and consistent evaluations, reducing variability among healthcare practitioners and institutions.DL models can swiftly and efficiently analyze big datasets, making them ideal for screening large populations. Early diagnosis of AD is critical for clinical trials and drug development activities. Identifying individuals in the early disease phases allows researchers to choose suitable candidates for testing prospective treatments and therapies to reduce or stop disease development (Cheung et al., 2022).

In summary, AD can be detected early through MRI methods, which are compared with normal brain activities to identify AD-related changes. DL, a subset of Artificial Intelligence and ML, is highlighted for its role in this process. DL involves creating complex ANNs that learn from vast data, akin to human brain functions. These networks, made of multiple interconnected nodes, can recognize intricate patterns without being explicitly programmed, drawing inspiration from the structure and function of the human brain.

1.1. Motivation

To address the challenges of AD Using MRI Data, this study introduces an ideal DL approach for early AD detection. The research

proposes various DL models: CNNs without-Aug, CNNs with-Aug, a blend of CNNs and Long Short-Term Memory (LSTM) with-Aug, mix of CNNs and SVM with-Aug, and a Transfer Learning method utilizing VGG16-SVM with-Aug. The effectiveness of the offered DL models is estimated by various evaluation metrics, including accuracy, specificity, precision, recall, F1-score, and processing time.

The study's methodology encompasses four primary stages. Initially, an appropriate AD dataset is gathered. The second stage involves data pre-processing, converting the obtained unstructured data into a structured format suitable for the classification process. Next, feature extraction and classification are conducted concurrently employing the provided DL models, as mentioned in earlier models. The final stage involves assessing these DL models' performance based on diverse pre-established assessment metrics. Based on this evaluation, the DL model that demonstrates superior performance is recommended for AD early detection.

1.2. Contributions

The paper presents an early detection approach for AD based on DL models. The main contributions that further emphasize the novelty of this proposed approach can be clarified in the following points:

- A new model, named AD-DL, is proposed aimed at early diagnosis and detection of AD, as well as binary classification of AD through DL methodologies.
- Five distinct DL architectures are proposed, which can be classified into two different strategies, namely without-Aug and with-Aug, specifically in the AD detection context.
- The proposed AD-DL model merges DL methods with ensemble learning, improving the accuracy and stability of its classification capabilities.
- The effectiveness of the recommended AD-DL models is confirmed by comparing their performance with current leading methods depending on established assessment metrics involving accuracy, specificity, precision, recall, F1-score, and processing time.
- Utilizing this AD-DL model, a 99.92%, 100.00%, 99.50%, 100.00%, and 99.70% for accuracy, precision, recall, specificity, and F1-score, respectively in classification are accomplished.
- An optimal balance is achieved between testing duration and detection effectiveness.

1.3. Paper organization

The rest of the paper is organized as follows. The related work is suggested in Section 2. The proposed model, the original CNN, and the three classifier models (LSTM and SVM) are shown in Section 3. Section 4 propose and analyze the experimental outcomes of the suggested AD-DL, the comparative models, and the managerial implication. The whole results are examined in Section 5. The conclusions and the future recommendations are concluded in Section 6.

2. Literature review

This section comprehensively reviews the pertinent literature, showcasing the pivotal role of ML and DL in medical research, with a specific focus on AD diagnosis. It highlights how advanced DL techniques are increasingly becoming integral in various stages of AD identification, particularly through imaging analysis. This review delves into the utilization of diverse feature extraction methods, spotlighting the automated frameworks that leverage biomarker techniques. It also examines the autonomous capabilities of DL in processing and extracting features from biomarkers, thereby creating sophisticated models adept at detecting AD and its progression stages. The section further explores commonly employed techniques in Alzheimer's classification, such as SVM, ANN, and deep neural network (DNN), underscoring the efficacy of DL in the diagnosis and classification of AD (Kishore and Goel, 2023; Diogo et al., 2022; Jo et al., 2019).

In 2016, Ortiz et al. (2016), applied DL method to distinguish between AD, MCI, and non-converting (NC) subjects. They utilized the Automated Anatomical Labeling (AAL) software to divide the brain into three-dimensional patches, which served as training data for their DNNs. The team employed four different voting algorithms in the prediction phase to enhance the model's accuracy. Their innovative approach resulted in an impressive classification accuracy of 90.00% in distinguishing NC from AD subjects. Following that, Sarraf and Tofighi (2016) employed CNNs to detect AD from brain MRI data. This type of medical information holds great significance as it serves as a basis for creating predictive models or algorithms that distinguish AD symptoms from those of healthy individuals and determine the phases of the disease. The authors utilized the ADNI dataset, comprising 43 images for validation, to conduct their research. With a mean accuracy of 96.85%, the authors could effectively diagnose AD using CNN.

After that, in 2018, Islam and Zhang (2018) developed a CNN model that utilizes brain MRI data to detect AD. They compared their model to other pre-trained DL approaches, such as ADNet, InceptionV4, and ResNet, using 416 photos from the OASIS dataset. Their approach outperformed earlier methods that relied on binary classification and provided the ability to differentiate between different stages of AD in early-stage diagnosis. The study results indicated that the CNN model surpassed the other approaches, achieving impressive performance metrics, involving accuracy, F1-score, precision, and recall, with values of 93.00%, 94.00%, 94.00%, and 92.00%, respectively.

And in 2019, Jo et al. (2019)in their study conducted a comparative study on the efficacy of traditional ML and DL methods in early AD detection and in predicting the advancement from Mild Cognitive Impairment (MCI) to AD. They examined 16 studies, where 4 combined traditional ML with DL, and 12 solely utilized DL. The combined approach yielded a 96.00% efficiency in feature selection and an 84.20% accuracy for predicting MCI to AD conversion. Specifically, using CNNs in DL achieved similar accuracies in feature selection and MCI to AD conversion prediction. The study also found that combining neuroimaging and fluid biomarkers could further enhance classification performance. Additionally, Lee et al. (2019) applied multimodal Recurrent Neural Networks (RNNs) to detect the progression from MCI to AD. They incorporated cross-sectional neuroimaging, longitudinal CSF analysis, and measurements of cognitive performance in their model to enhance predictive accuracy. The research demonstrated that while a single modality led to 75.00% accuracy, integrating multiple modalities improved this to 81.00%. Following that also, Ahmed et al. (2019) utilized MRI scans to develop a streamlined CNN framework aimed at detecting AD, specifically focusing on the left and right hippocampal regions. To validate their approach, they employed both the Gwangju Alzheimer's and Related Dementias (GARD) dataset and the ADNI dataset as separate validation sets, ultimately analyzing a combined total of 352 GARD MRI scans and 326 ADNI MRI images.

In 2020, Yang and Liu (2020) and Rolls et al. (2020) have developed a DL algorithm focuses on the early-stage forecast of Alzheimer's employing fluorine Fluorodeoxyglucose PET scans. This approach, employing the CAFFE DL framework, led to the development of accurate prediction and classification models. The Convolutional Architecture for Fast Feature Embedding (CAFFE) extracted features from FDG PET images, effectively classifying MCI stage features and expecting their progression. Both healthy people's and AD sufferers' scans were confidently evaluated using the generalized matrix learning vector quantization. The study also incorporated hierarchical 2D CNN for intra-slice information collection and a Gated Recurrent Unit (GRU) RNN for inter-slice feature extraction. This method achieved high classification performance, as evidenced by impressive AUC values in differentiating AD from normal cognition (NC) and MCI from NC. A novel contrastive-based learning strategy was applied to overcome challenges in PET image analysis. This method amplified sections of 3D

PET images and used contrastive loss to enhance feature differentiation between classes and reduce intra-class variations. It involved a dual-layer convolutional module for improved visual domain recognition. Also, in the research conducted by Pan et al. (2020a,b), they have developed the application of DNNs in FDG-PET imaging for early AD detection. The MiSePyNet network, effective in learning from multiple views of PET scans, merged these representations seamlessly, enhancing reliability. The method employed separable convolution to maintain spatial information and reduce training parameters, deviating from traditional 3D convolution methods for 3D image processing, which are more complex and resource-intensive. They also employed a CNN model in conjunction with ensemble learning (EL) to diagnose AD through MRI data analysis in their study. Utilizing 278 images from the ADNI dataset, they compared their approach to other methods, including 3D-SENet and PCA + SVM. The trial results demonstrated that the combination of CNN and EL was the most effective, achieving an accuracy rate of 85.00%.

Following that, Shi et al. (2020) introduce a new approach for identifying individuals with AD versus those who are healthy, based on functional connectivity (FC) among brain activity voxels. The research indicates that FC patterns between voxels in the prefrontal lobe and between the prefrontal and parietal lobes are key factors in predicting AD patients with higher accuracy. This technique shows great promise for future applications in the field. Also, Bae et al. (2020) utilized MRI images from a diverse range of individuals regarding race, education level, age, and gender to create a CNN-based approach for detecting AD. To ensure accuracy, they drew upon two separate datasets — one from Seoul National University Bundang Hospital (SNUBH) and the other from the ADNI dataset. This allowed them to achieve an average classification accuracy of 88.00%–89.00% and a sensitivity of 85.00%–88.00% using 195 images from each dataset. The estimated processing time per individual was around 23–24 s. In 2021, Helaly et al. (2021) explored various techniques for categorizing medical images and detecting AD. The first approach involved implementing CNN architectures to process 2D and 3D structural brain scans from the AD Neuroimaging Initiative (ADNI) dataset, using 2D and 3D convolutions. The results demonstrated that using CNN, the accuracy rates for multi-class AD phase categorization were 95.17% for 3D and 93.61% for 2D scans. The researchers used the pre-trained VGG19 model for the second method, achieving a multi-class classification accuracy of 97.00% when analyzing longitudinal brain MRI data. Additionally, Following that, Battineni et al. (2021) has developed a mechanism to identify patients with dementia and differentiate between those with AD and other illnesses. The study used a sample of 150 individuals from the OASIS dataset to validate their findings. Six supervised classifiers, including gradient boosting, SVM, logistic regression, random forests, Ada-Boosting, and naive Bayes, were combined using 10-fold cross-validation to classify AD. The results indicated that the gradient boosting method had the highest accuracy, at 97.58%, and a recall of 96.00%, outperforming the other classifiers.

In 2022, van Veen et al. (2022) in their study, they have developed DL algorithms for precise clinical diagnosis from FDG-PET brain scans, enabling a reliable comparison with conventional clinical methods in identifying AD, MCI, or non-dementia cases. These algorithms enhance diagnostic accuracy by detecting subtle features overlooked in standard clinical image examinations. Additionally, Subramoniam et al. (2022) have developed a model using sliced MRI images as inputs for residual CNNs (ResNet-101) to extract features and classify dementia stages. Their model successfully categorized images into four classes: moderately demented, mildly demented, very mildly demented, and non-demented. They achieved a high accuracy of 95.32% using a combination of three layers of CNN and three layers of Vanilla-dense neural network, with specific activation functions. Edward Challis and his team compared SVM classifiers with Gaussian process logistic regression (GP-LR) and found GP-LR more effective in certain scenarios. This research contributes to understanding and diagnosing AD, a progressive neurodegenerative condition where early detection is vital for managing symptoms and risks. The study highlights the effectiveness of advanced imaging and ML techniques in this area. Also, in the research conducted by Bhadra and Kumar (2022), they proposed statistical examinations of various ML and DL models developed by researchers for specific applications. It delved into the diverse techniques and methods employed in these models, analyzing their effectiveness and areas of use. The analysis included a range of modalities and approaches utilized within the field, providing insights into the advancements and innovations in machine and DL research. Alnaim and Alwakeel (2023) used a distributed-edge-computing-based IoT framework, combined with machine learning, to effectively handle the vast data generated by medical sensors. Their focus was on enhancing real-time responses, optimizing data transfers, and ensuring privacy and security in IoT devices, aiming to improve network efficiency and computation decentralization in healthcare applications.

Following that, Alorf and Khan (2022) focused on classifying various stages of AD using resting-state functional MRI (rs-fMRI) and DL. AD, known for progressively impairing cognitive abilities, has been traditionally diagnosed through binary classification methods distinguishing it from MCI. However, there is a gap in research regarding the detailed classification of AD's advancing phases. Addressing this, the research introduces methods for multi-label classification of six Alzheimer's stages, utilizing rs-fMRI data. The approach involved extracting the brain's FC networks from rs-fMRI and implementing two DL techniques: Stacked Sparse Autoencoder and Brain Connectivity Graph Convolutional Network. The models' performance was evaluated through k-fold cross-validation, achieving an average accuracy of 77.13% with Stacked Sparse Autoencoders and 84.03% with Brain Connectivity Convolutional Network. The study also included an analysis of significant brain regions implicated in AD, leveraging the networks' learned weights. Key areas identified include the precentral gyrus, frontal gyrus, lingual gyrus, and supplementary motor area. This research contributed to a deeper understanding of AD progression and offers new diagnostic and research possibilities through advanced neuroimaging and DL applications.

In 2023, Shukla et al. (2023) developed DL algorithm to identify AD using a dataset of 6219 MRI images depicting the brain at different cognitive impairment and hallucination stages. Various DL techniques were employed, including CNN, DenseNet121, ResNet101, and VGG16. CNN emerged as the most effective technique, with an accuracy of 97.00% and a recall of 97.60%, accompanied by a low loss of 0.091. Also, Sethuraman et al. (2023) proposed a state-of-the-art automated diagnosis system for AD. The system combines customized deep-learning models and effectively distinguishes AD from normal cognitive conditions. With an accuracy of 96.61%, this model shows great potential in diagnosing and treating AD. After that, Wang et al. (2023) aimed to discover new diagnostic biomarkers for AD using metabolomics data from Ultra Performance Liquid Chromatography Mass Spectrometry (UPLC-MS/MS) for developing DL predictive tools. It involved 177 individuals, including 78 AD patients and 99 cognitively normal (CN) participants, from the ADNI cohort. The research utilized 150 metabolomic biomarkers, and feature selection was conducted using the Least Absolute Shrinkage and Selection Operator (LASSO), which identified 21 significant metabolic biomarkers. These biomarkers were used to construct multilayer feedforward neural networks through the H2O DL function, dividing the data into 70.00% for training and 30.00% for validation. The most effective DL model featured two layers and 18 neurons, achieving an accuracy of 88.10%, F1-score of 89.20%, and AUC of 87.30%. Key findings highlighted the role of metabolomic biomarkers in glucose and lipid metabolism, particularly bile acid metabolites, and their association with genetic and clinical markers of AD, cognitive assessments, and hippocampus volume. The study concluded that the new metabolomic biomarkers

were promising for early AD diagnosis, risk stratification, and early intervention in at-risk patients.

Additionally, Kishore and Goel (2023) aimed to develop a DNN for diagnosing AD and categorizing its stages using Fluorodeoxyglucose PET scans. FDG-PET is an effective diagnostic tool for detecting glucose metabolism anomalies in the brains of AD patients. The researchers created a DNN to differentiate between subjects with AD, stable MCI (sMCI), progressive MCI (pMCI), and CN individuals. They collected a total of 83 FDG-PET scans from the ADNI database, comprising 21 CN subjects, 21 sMCI subjects, 21 pMCI subjects, and 20 AD subjects. The method achieved exceptional accuracy rates: 99.31% for CN versus AD, 99.88% for CN versus MCI, 99.54% for AD versus MCI, and 96.81% for pMCI versus sMCI. These results demonstrate the proposed method's significant generalization ability and its effectiveness in predicting the conversion of MCI to AD, even without direct information. The study concludes that FDG-PET, a well-known biomarker, can effectively identify AD using transfer learning in DNNs. This approach shows promise for improving diagnostic accuracy and early detection of AD and its various stages.

Based on the previous studies, it can be said that the data size is relatively small. Furthermore, the outcomes may be more suitable for dealing with medical data. Dealing with human life, medical, and disease data is delicate and demands high accuracy. As a result, these issues will be addressed in this study by working with larger data sets and generating results that are more accurate and superior. Consequently, this work aims to investigate and compare multiple DL models for early AD diagnosis to find the best DL model among them that performs better than previous studies in the same field. Section 3 describes using two strategies to implement distinct DL models.

3. Proposed model

The paper describes a unique approach for detecting early on using binary techniques. The approach is made up of several phases, as shown in Fig. 1. MRI pictures go through a preprocessing pipeline in the first data preparation phase, including data resizing, labeling, normalization, and color modification. In the second phase, training and testing sets are created from the preprocessed data, which are utilized to develop and train the proposed DL models. The third phase is the study of the DL models to suggest DL models include tasks for automated feature extraction and classification. Additionally, the study suggests CNNs-without-Aug, CNNs-with-Aug, CNN-LSTM-with-Aug, CNNs-SVM-with-Aug, and Transfer learning using VGG16-SVM-with-Aug. The principal purpose of using these models is to discover the one that delivers the best balance of testing time and detection accuracy.

3.1. CNNs-without-Aug

The CNN is a form of binary perceptron (Yamashita et al., 2018). Unlike a basic neural network, a CNN can learn complicated features, making it extremely useful in image classification, object recognition, and medical picture analysis. A CNN's core premise is its capacity to extract local features from higher-level inputs and move them down to lower layers for more intricate feature representation. A CNN incorporates convolutional, pooling, and fully connected (FC) layers. Fig. 2 depicts a standard CNN architecture with these layers.

A set of kernels is incorporated in the convolutional layer to produce a tensor of feature mappings. These kernels employ strides to convolve the full input, producing output volume dimensions that are integers. The striding procedure causes the dimensions of the input volume of the convolutional layer to be reduced. In order to keep the input volume's size with low-level features, zero padding is essential to pad an input volume with zeros. The convolutional layer's equation is as follows:

$$F(i,j) = (I \times K)(i,j) = \sum \sum I(i+m, j+n)K(m,n). \quad (1)$$

where, F is a 2D feature map's output , I is the input matrix, and K is a 2D filter with a size of $m \times n$. $I \times K$ stands for the convolutional layer's operation. The Rectified Linear Unit (ReLU) layer is used to increase non-linearity in feature maps. ReLU computes activation by maintaining a zero threshold input. It is represented mathematically in the following equation:

$$f(x) = max(0, x). \quad (2)$$

To lessen the parameter number, the pooling layer downsamples an input dimension that has been specified. The most often used method, max pooling, produces the highest value within a given input. The FC layer is employed as a classifier to categorize data from the convolutional and pooling layers. The CNN model was employed with multiple convolutional and pooling layers to extract features from the preprocessed photos. The model has the following layers:

- Rescaling layer: This preprocessing layer rescales the input values to a new range. The scale was set to 1/255, which converts the input from [0, 255] to [0, 1]. The rescaling layer gets an input tensor with the shape (224, 224, 3), and its output shape matches the input shape.
- Convolutional layer (Con2D): This layer employs 16 filters of size $3 * 3$ and employs the ReLU activation function, as mathematically represented in Eq. (2).
- Max-pooling layer (MaxPooling2D): This layer selects the maximum output value within a neighborhood specified by a pool size of $2 * 2$. As previously said, it lowers the spatial dimensionality of the feature maps created by the convolutional layer. If an activation map has a size of W * W * D, a pooling kernel of spatial dimension F, and a stride S, the size of the output volume can be calculated using the following formula:

$$\text{Output size} = \frac{W - F}{S} + 1. \quad (3)$$

- Another Convolutional layer: This layer is made up of 32 filters of size $3 * 3$ that use the ReLU activation function.
- Another max-pooling layer is used, this time with a pool size of 2 *2.
- Dropout layer: A 0.25 dropout rate dropout layer is used. Dropout prevents overfitting by randomly setting the outgoing edges of concealed units to 0 during training. A dropout rate of 0.25 indicates that there is a 25.00% possibility that the output of a specific neuron will be driven to 0.
- Another convolutional layer: This layer has 64 filters with $3 * 3$ size and uses the ReLU activation algorithm.
- Another max-pooling layer is implemented: A max-pooling layer with a pool size of $2 * 2$ is used.
- Another dropout layer: The probability of this dropout layer is 0.20.
- Flattened layer: The flattened layer turns the previous layer's 2D feature maps into a 1D vector.
- Dense layer: With 128 units and the ReLU activation function, this completely connected layer is dense. It takes into account all input neurons for each output neuron.
- Another dense layer: This dense layer has 64 units and is activated by the ReLU function.
- The last dense layer is made up of 2 units and uses the softmax activation function. The softmax function generates a probability distribution over two classes, with values ranging from 0 to 1 and adding up to 1. It can be stated numerically as the following equation :

$$f_j(Z) = \frac{e^Z j}{\sum_k e^Z k}. \quad (4)$$

Z represents a vector of values in this equation, and $f_j(Z)$ computes the exponential of the $(j - th)$ element of Z divided by the

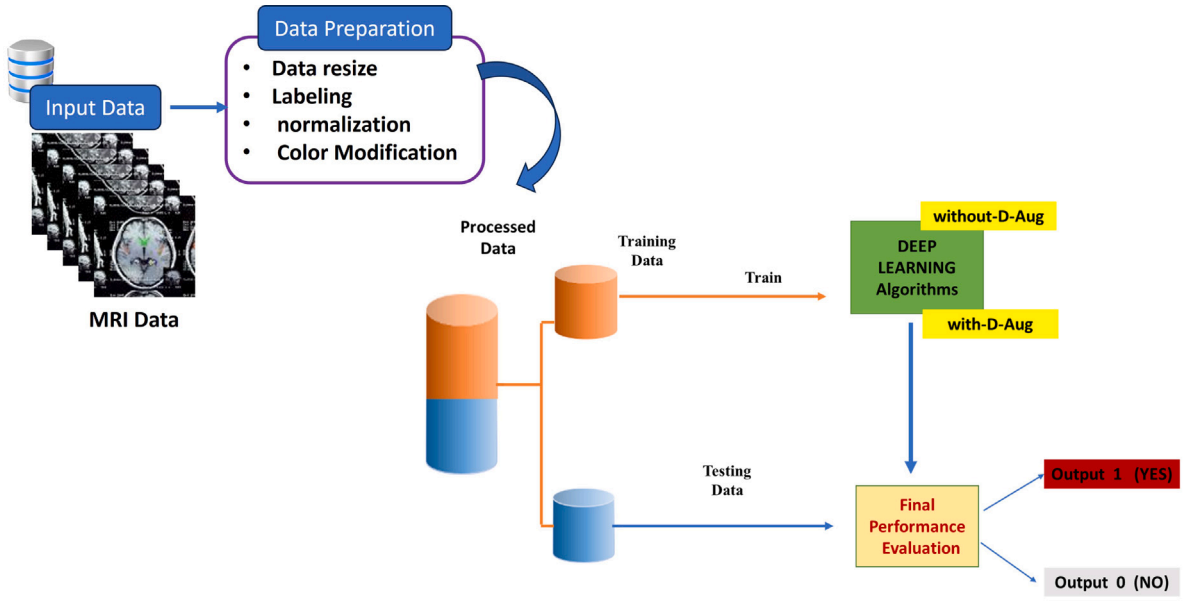

Fig. 1. The proposed model for early detection of AD.

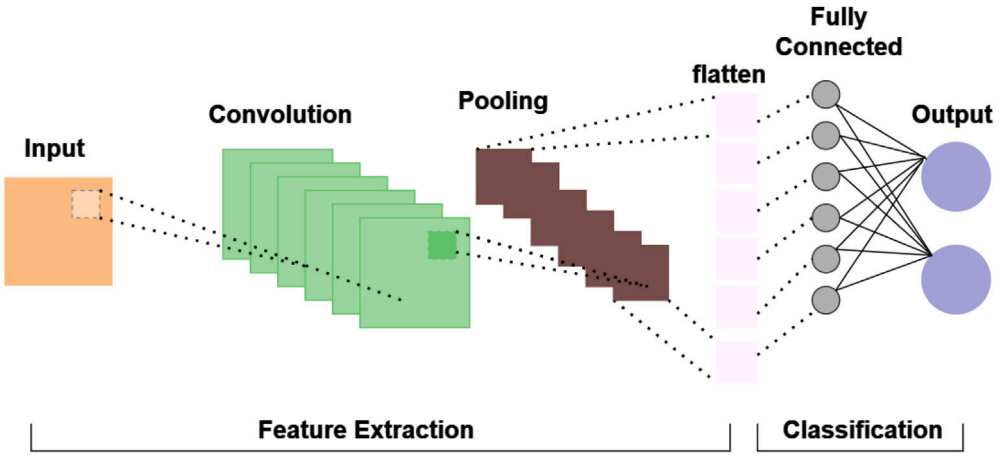

Fig. 2. CNN architecture.

total of the exponentials of all elements in Z. This ensures that the output values span from 0 to 1 and add up to 1, resulting in a probability distribution.

Overall, the proposed CNN model architecture has 13 layers in total, as shown in Fig. 3

3.2. CNNs-with-Aug

Data augmentation is a method utilized to extend a dataset by implementing diverse changes to current data, resulting in the creation of additional samples (Helaly et al., 2021; Battineni et al., 2021; Sarraf and Tofighi, 2016). The primary objective of augmentation is not only to augment the sample count of the dataset but also to provide diverse variants that mitigate the risk of overfitting and improve the model's capacity to generalize when confronted with unfamiliar images. In order to implement Data Augmentation, the ImageDataGenerator module from Keras is employed, which provides a convenient method for supplementing data without incurring substantial computational costs. By utilizing the ImageDataGenerator, batches of tensor image data are successfully generated in real-time, integrating data augmentation techniques. This methodology ensures that the proposed model is exposed to a wide range of data fluctuations in every iteration, effectively mitigating the risk of overfitting. In addition, using ImageDataGenerator enhances memory efficiency by loading images in groups instead of all images simultaneously. The study used specific augmentation methods, including random picture rotations spanning from 0 to 90 degrees, random horizontal and vertical flips, random magnification, and random shifting of images. In this study, the CNN model is employed, as recommended in Fig. 3, making minor adjustments to the input shape (128, 128, 3) and the Dropout layers to be as in Fig. 4. The outcomes section, as depicted in Fig. 4, showcases the performance of the model above, incorporating the aforementioned modifications when supplemented by data augmentation. The model has the following layers:

- The first layer in the model design is the Rescaling layer, which is responsible for performing preprocessing tasks. The function of this layer is to transform the input values to a different range. In this particular instance, a scaling factor of 1/255 has been established, which serves to convert the input values from the interval [0, 255] to the interval [0, 1]. The Rescaling layer accepts an input tensor of dimensions (128, 128, 3) and preserves the same shape for its output.

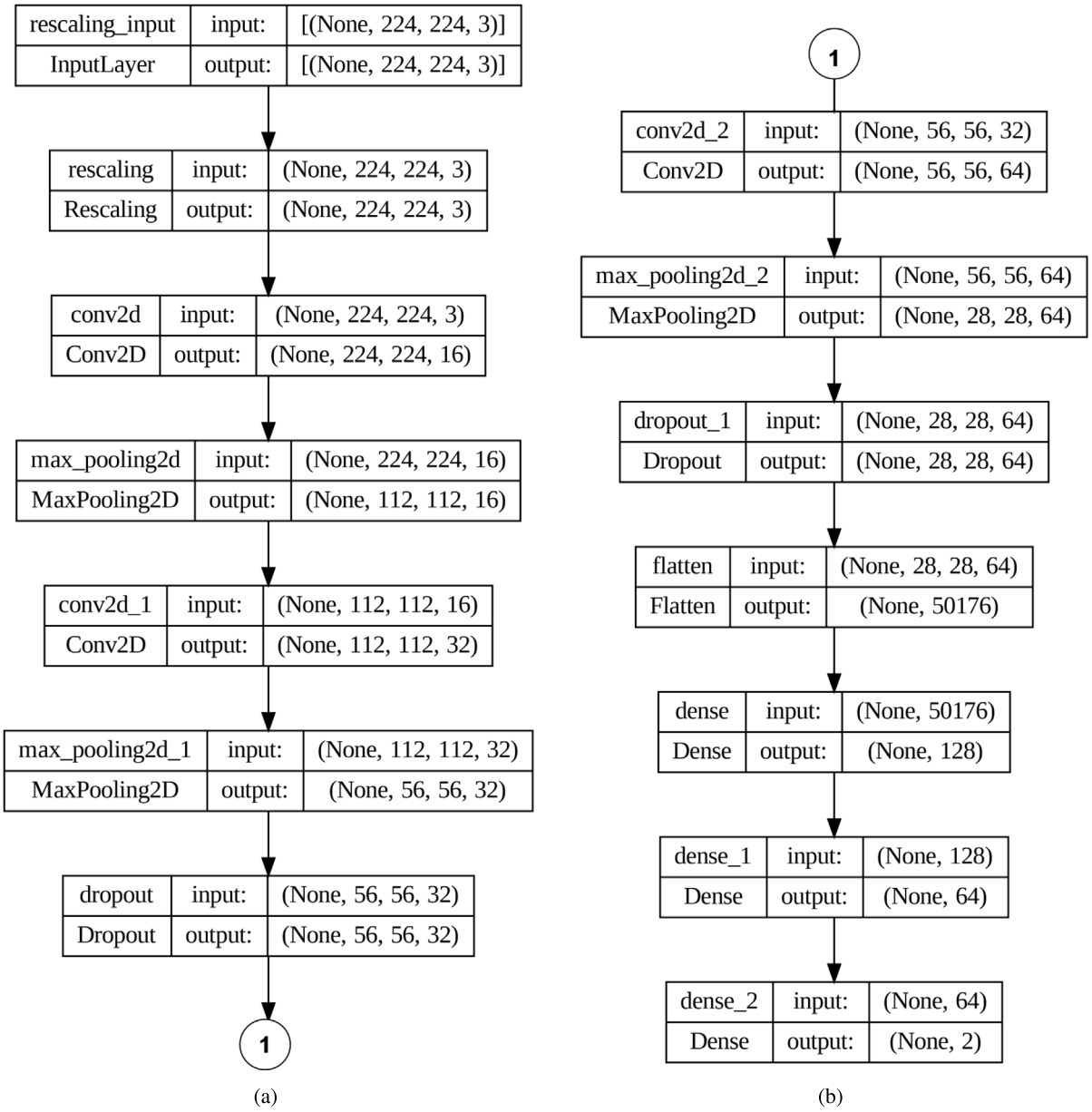

Fig. 3. The suggested model architecture of CNNs-without-Aug.

- The subsequent layer consists of a Convolutional layer (Conv2D) including 16 filters measuring 3 × 3 in size. The ReLU activation function is utilized, as denoted by Eq. (2).
- Subsequently, a max-pooling layer (MaxPooling2D) is employed with a pool size of 2 × 2, as represented mathematically by Eq. (3).
- The subsequent layer is a convolutional layer that consists of 32 filters, each with a size of 3 × 3. This layer employs the ReLU activation function.
- Following this, there is an additional layer of max-pooling (MaxPooling2D) implemented with a pool size of 2 × 2.
- The sixth layer is implemented as a dropout layer with a dropout rate 0.20. Dropout is a method employed to mitigate the issue of overfitting in models. During each training phase update, this system randomly assigns a value of zero to the outbound connections of hidden units, neurons located within hidden layers. A dropout rate of 0.20 signifies that there is a probability of 20.00% for each concealed unit to be randomly assigned a value of zero. In alternative terms, it might be stated that there exists a 20.00% likelihood that the output of a certain neuron will be compelled to assume a value of zero.
- The subsequent layer, known as the seventh layer, consists of a convolutional layer that utilizes 64 filters of dimensions 3 × 3. This layer employs the ReLU activation function.
- Subsequently, a subsequent layer of max-pooling (MaxPooling2D) is implemented, utilizing a pool size of 2 × 2.
- The ninth layer consists of an additional dropout layer with a dropout rate of 0.25.
- The tenth layer is a flattened layer, denoted as "Flatten", which transforms the two-dimensional feature maps obtained from the preceding layer into a one-dimensional vector representation.
- Following that, there is a densely connected layer (referred to as Dense) with 128 units and employing the ReLU activation function. The layer under consideration is characterized by complete connectivity, wherein every output neuron incorporates information from all input neurons.

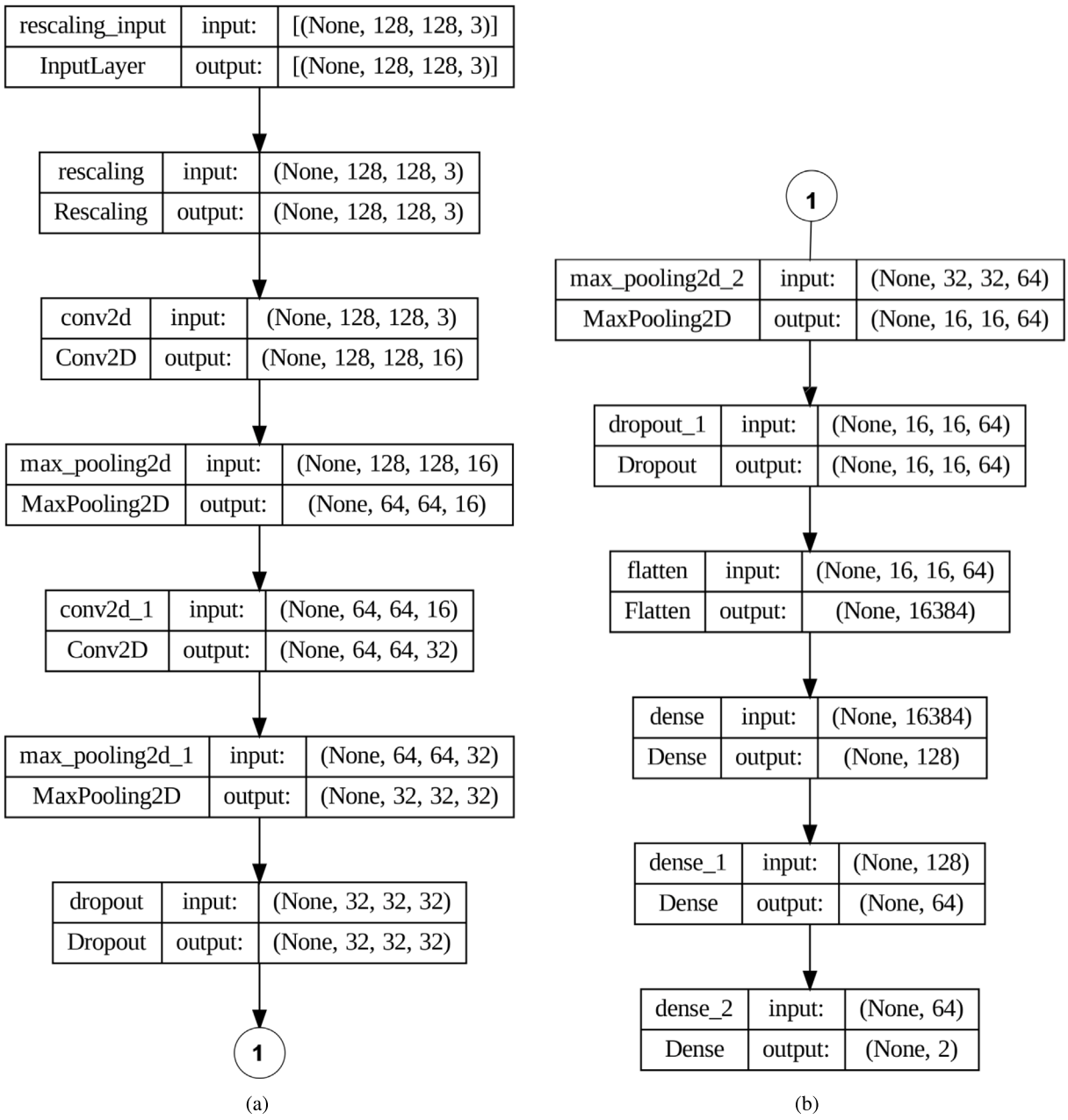

Fig. 4. The suggested model architecture of CNNs-with-Aug.

- The subsequent layer, known as the twelfth layer, is a densely connected layer (Dense) consisting of 64 units and utilizes the ReLU activation function.
- The ultimate layer consists of a dense layer (Dense) comprising 2 units, employing the softmax activation function. The output of this layer is a probability distribution encompassing two classifications within the dataset. The softmax function is a mathematical operation that converts a vector of K real values into another vector of K real values, ensuring that the elements of the resulting vector add up to 1. The input values encompass a range of possibilities, including positive, negative, zero, or values higher than one. However, the softmax function is employed to standardize these input values, ensuring that they fall within the range of 0 to 1. The mathematical representation is given by Eq. (4).

Overall, the suggested CNN model architecture of CNNs-with-Aug is shown in Fig. 4

3.3. CNNs-LSTM-with-Aug

This section will comprehensively elucidate the operational mechanisms of LSTM. Subsequently, the process of integrating LSTM with CNNs will be explicated in order to facilitate the preparation for tasks related to image classification. The LSTM architecture, specifically the one denoted as LSTM (Yu et al., 2019; Staudemeyer and Morris, 2019; Smagulova and James, 2019), has been developed to improve the performance of RNNs by mitigating the problems of gradient vanishing and exploding. Instead of utilizing traditional RNN units, LSTM offers memory blocks as a proposed solution. The primary differentiation between LSTM and RNNs resides in including a cell state, which enables long-term information retention. The LSTM network can effectively retrieve and integrate information from earlier time steps to the current time step. The system consists of three gates: an input gate, a "forget" gate, and an output gate. The present input is symbolized as x_t, while

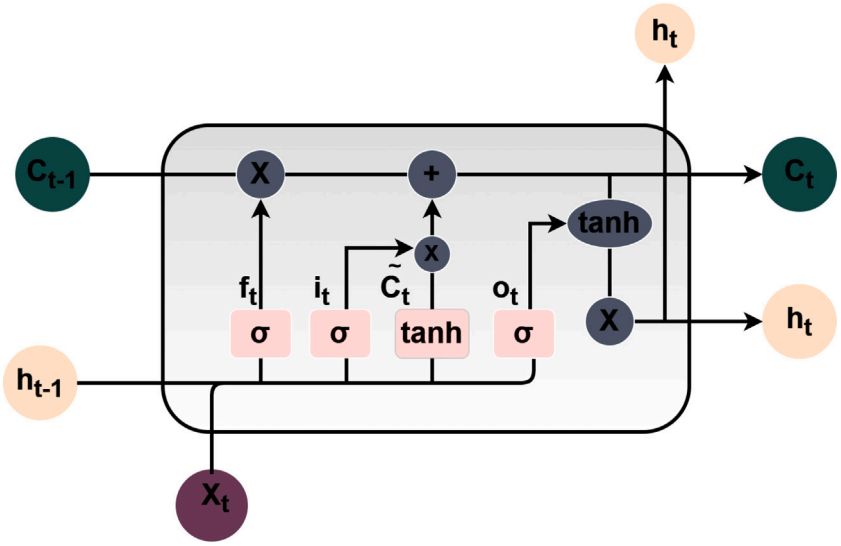

Fig. 5. LSTM architecture.

the preceding and updated cell states are indicated as c_{t-1} and c_t, correspondingly. The present and previous outputs are denoted as h_t and h_{t-1}, respectively. The interior architecture of the LSTM model is depicted in Fig. 5.

The subsequent equations illustrate the input gate's operational principle in LSTM:

$$i_t = \sigma(W_i \cdot [h_{t-1}, x_t] + b_i), \tag{5}$$

$$\tilde{C}_t = \tanh(W_i \cdot [h_{t-1}, x_t] + b_i), \tag{6}$$

$$C_t = f_t C_{t-1} + i_t \tilde{C}_t, \tag{7}$$

$$f_x = \frac{1}{1+e^{-x}} = \frac{e^x}{e^x+1}, \tag{8}$$

$$f_x = \frac{e^x - e^{-x}}{e^x + e^{-x}}, \tag{9}$$

$$f_t = \sigma(W_f \cdot [h_{t-1}, x_t] + b_f). \tag{10}$$

where Eq. (5) is utilized to quantify the degree to which information from h_{t-1} and x_t is integrated. The objective above can be accomplished by subjecting these values to a sigmoid layer, as denoted by Eq. (8). Subsequently, the previous hidden state h_{t-1} and the current input x_t undergo a hyperbolic tangent activation function, denoted as a tanh layer, which can be mathematically expressed as Eqs. (9) and (6) is then used to gain additional information. The output obtained from the hyperbolic tangent layer is represented as $\tilde{C}_t$. The equation denoted as (7) integrates the data from the present input, $\tilde{C}_t$, and the previous long-term memory, $\tilde{C_{t-1}}$, in order to modify the existing cell state, $\tilde{C}_t$. The symbols W_i and b_i are used to denote weight matrices and the bias term of the input gate in the context of LSTM networks. The selective transmission of information is facilitated by incorporating a sigmoid layer, dot product, and the forget gate inside the LSTM architecture. Eq. (10) integrates the weight matrix W_f, offset b_f, and sigmoid function to ascertain the decision of whether to discard pertinent information from the preceding cell, contingent upon a certain probability. To summarize, Eqs. (5)–(10) are fundamental components within the LSTM architecture. These equations are responsible for governing the processes of input integration, selective transmission, and probable forgetting of prior cell state information. The states needed for continuance by the h_{t-1} and x_t inputs following Eqs. (11) and (12) are specified by the output gate of LSTM. The state decision vectors that convey new information, C_{t-1}, across the tanh layer are found and multiplied to get the final output.

$$O_t = \sigma(W_o \cdot [h_{t-1}, x_t] + b_o), \tag{11}$$

$$h_t = O_t \tanh(C_t), \tag{12}$$

where W_o and b_o are the output gate's LSTM bias and weighted matrices, respectively.

The equation referenced pertains to the LSTM architecture, a variant of RNN models. The calculation of the hidden state at a specific time step in an LSTM cell is represented by the equation: The equation for the hyperbolic tangent function is given Eq. (12). The following is an analysis of the equation: The variable h_t denotes the concealed state or output at a specific time step, denoted as t. The statement above encapsulates pertinent data from previous observations and exerts an impact on future prognostications. The term O_t refers to activating the output gate at a specific time step, denoted as t. The output gate is responsible for regulating the extent to which the memory of the cell is made accessible to either the subsequent layer or the output. The computation is performed by considering the present input and the preceding hidden state. Cell state, indicated by C_t, refers to the state or memory of a cell at a specific time step, denoted as t. The cellular state is accountable for storing and transmitting information across various temporal intervals. The LSTM model possesses the capability to make selective decisions regarding the retention or omission of information, which is contingent upon both the input and the activation of the gating mechanisms. The hyperbolic tangent activation function, commonly denoted as tanh, is a mathematical function used in several fields, such as ML and neural networks. The cell state values are compressed within the interval of −1 to 1. The utilization of this activation function facilitates the regulation of information propagation within the cell state. The equation supplied allows for the computation of the latent state at a given time step, t, by considering the activation of the output gate and the current cell state. The statement above encapsulates the primary mechanism through which information is transmitted within an LSTM cell.

The hybrid CNNs-LSTM-with-Aug model, which is being suggested, employs a fusion of CNNS and LSTM networks in order to do image categorization. The model comprises multiple layers that provide distinct roles as follows:

- The initial layer consists of a Conv2D layer with 64 filters, each having a size of 3 × 3. The activation function used in this layer is the ReLU. The input tensor has a shape of (1, 128, 128, 3), which corresponds to a single-color image with a size of 128 × 128.

- The subsequent layer is a max-pooling layer, specifically MaxPooling2D, which employs a pool size of 2 × 2.
- The subsequent convolutional layer undergoes a reduction in spatial dimensions through the implementation of this particular layer.
- The subsequent layer is a convolutional layer (Conv2D) consisting of 32 filters, each with a size of 3 × 3, and utilizing the ReLU activation function.
- The subsequent layer in the architecture is a max-pooling layer (MaxPooling2D) with a pool size of 2 × 2.
- The fifth layer is a flattening layer, denoted as "Flatten", which transforms the two-dimensional feature maps obtained from the preceding layer into a one-dimensional vector representation.
- The sixth layer consists of a LSTM layer of 100 units and employs default hyperparameters. The function of this layer is to act as a classifier for the model.
- The ultimate layer consists of a dense layer, specifically a dense layer, comprising 2 units and utilizing the sigmoid activation function. The algorithm generates a probability distribution encompassing the dataset's two classes.

The overall architecture of the hybrid CNNs-LSTM-with-Aug model comprises a total of seven layers. These layers encompass two convolutional layers, two max-pooling layers, a flattening layer, an LSTM layer, and a dense layer. The LSTM layer is preceded by multiple time-distributed layers, which serve as wrappers enabling the application of a layer to each individual temporal slice of the input. This feature proves to be highly advantageous when dealing with image inputs and harnessing the memory capabilities of the LSTM network. Consult Fig. 6 in the included reference for a graphical depiction of the model's construction.

3.4. CNNs-SVM-with-Aug

The classification of photographs has emerged as a significant subject in the contemporary era, with the objective of precisely assigning descriptive labels to visual content. CNNs are frequently utilized in the field of image categorization, a well-accepted and viable methodology. However, one may come across inquiries regarding the application of conventional ML methods, such as SVMs, in the context of picture categorization.

The SVM is a well-established classification technique capable of effectively addressing classification and regression problems. The software adeptly manages a wide range of variables, encompassing both continuous and categorical types. The SVM algorithm constructs a hyperplane within a multidimensional space to classify distinct classes effectively. By means of an iterative procedure, an ideal hyperplane is constructed in order to minimize errors. The main goal of SVM is to determine the Maximum Marginal Hyperplane (MMH) that optimally classifies the given dataset. Hence, although CNNs are widely utilized for picture classification, it is prudent to contemplate the utilization of SVMs due to their distinctive skills in managing classification jobs and their potential effectiveness in specific situations. This paper focuses on a binary classification issue comprising four distinct classes. Hence, the squared hinge loss function and softmax activation function are employed in constructing the SVM model. The proposed model, which combines CNNs with SVMs and data augmentation techniques, integrates convolutional and pooling layers to extract relevant characteristics from preprocessed photos. Following that, the CNN's output layer is transformed into SVM classifier, as elucidated earlier. The proposed hybrid model architecture, which combines CNNs with SVMs and data augmentation techniques, consists of the following layers:

- The initial layer consists of a Conv2D layer with 64 filters, each having a size of 3 × 3. The activation function used in this layer is the ReLU. The model accepts an input tensor with dimensions of (224, 224, 3).
- The subsequent layer is a max-pooling layer, specifically MaxPooling2D, which employs a pool size of 2 × 2.
- The subsequent convolutional layer is responsible for decreasing the spatial dimensions of the feature maps acquired from the preceding layer.
- The subsequent layer is a convolutional layer (Conv2D) consisting of 32 filters, each with a size of 3 × 3, and utilizing the ReLU activation function.
- The subsequent layer in the architecture is a max-pooling layer (MaxPooling2D) with a pool size of 2 × 2.
- The fifth layer is a flattening layer, denoted as Flatten, which transforms the two-dimensional feature maps obtained from the preceding layer into a one-dimensional vector representation.
- The last layer of the model consists of a dense layer, namely a dense layer, with a total of 2 units. This dense layer is then transformed into a SVM layer through the use of a kernel regularizer and the utilization of L2 normalization. The softmax activation function is applied to the output layer, as denoted by Eq. (4). Furthermore, the squared hinge loss function is utilized in the process of model compilation.

Overall, The proposed architecture for the hybrid CNNs-SVM-with-Aug model comprises a total of six layers. These layers include two convolutional layers, two max-pooling layers, a flattening layer, and an output layer, which is a dense layer that is then transformed into an SVM layer. Fig. 7 For a visual depiction of the model architecture.

3.5. Transfer learning using VGG16-SVM-with-Aug

The utilization of the VGG16 model (Rohini, 2021) is employed to extract characteristics from MRI data. The VGG16 architecture comprises several layers, commencing with a convolutional layer. The first input to the primary convolutional layer consists of an image with dimensions of 224 × 224 pixels. The image is subjected to a sequence of convolutional (conv) layers that employ specialized filters for processing. The ReLU serves the dual purpose of functioning as a nonlinear activation function and as a convolutional layer. The architectural design comprises a total of 13 convolutional layers, 5 MaxPooling layers, and 3 fully linked layers. The VGG-16 architecture comprises 16 layers, 13 convolutional layers, and 3 fully linked layers, which justify its name. The model incorporates a softmax layer at the final output to facilitate classification. The transfer learning technique is implemented by utilizing the pre-trained VGG16 model to enhance the training's efficiency. The architectural depiction of VGG16 is presented in Fig. 8 and Fig. 9. The proposed approach (Desai et al., 2021; Tun et al., 2021; Ahmed et al., 2023) removes the final layer of VGG16 to extract characteristics from alternative layers, as illustrated in Fig. 10. Following this, various ML methods, particularly SVMs, are utilized for the classification stage in the presented model, as depicted in Fig. 11.

4. Experimental results

In this section, The work presented includes the suggested models' analysis and experimental findings. The assessment of the models encompassed the utilization of training and testing datasets, with the ultimate outcomes being determined by the mean value of all evaluation criteria. The duration allocated to training and tests was also documented. The evaluation of the proposed model's performance was conducted using specified datasets, as outlined in Section 4.1. The details about workplace characteristics are outlined in Section 4.3, whereas in Section 4.4, a comparison analysis is presented.

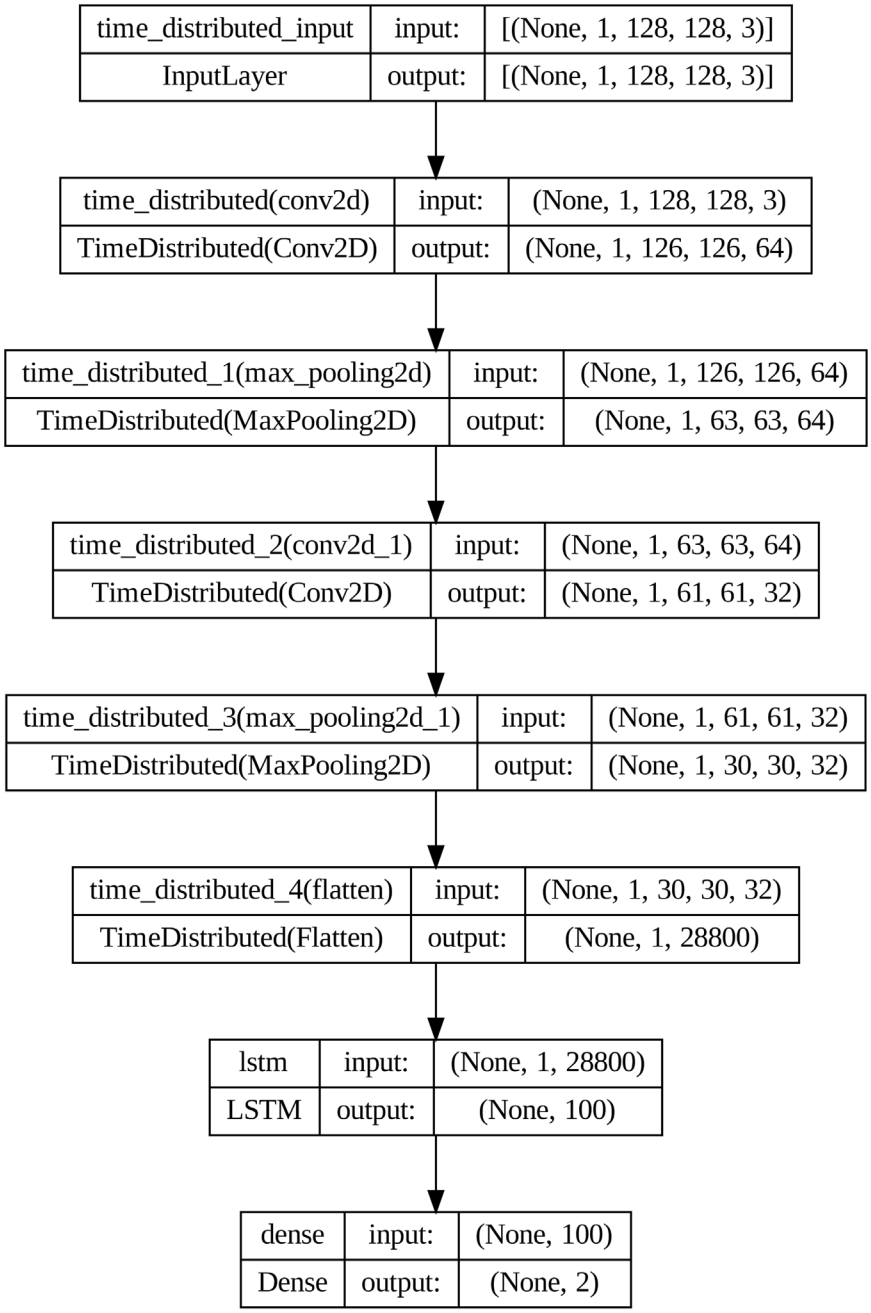

Fig. 6. CNN-LSTM-model.

4.1. Description of the dataset

To evaluate the proposed models in comparison to state-of-the-art models, data obtained from the MRI scans of the ADNI 1,[1] were employed. The dataset utilized in this research, sourced from Kaggle, includes a total of 6400 MRI images classified into four distinct classes: Mild-Demented, Moderate-Demented, Very-Mild-Demented, and Non-Demented. Table 1 shows the total number of images in the dataset. For the proposed models, it is binary classification. So, the classes of data combined into two classes, Demented and Non- demented; Mild-Demented, Moderate-Demented, and Very-and Mild-Demented, are combined together as Demented and Non-Demented as it is as in Table 2. Fig. 12 shows a visualization sample of the data. To maintain uniformity in terms of size, quality, and color, the photos within the dataset were subjected to preprocessing procedures, including resizing and color alteration. Subsequently, a normalization technique was employed to ensure that all pixels were scaled to a consistent range. The photos were appropriately labeled, with the designation "0" denoting Non-Demented and "1" denoting Demented. The dataset underwent a shuffling process, resulting in a division of 80.00% for training purposes, including 5120 photos, and 20.00% for testing purposes, encompassing 1280 images.

4.2. Working environment

The simulation results were generated using a Google collab. A suite of programming tools, including Python, Keras, Tensorflow, and

[1] https://www.kaggle.com/datasets/tourist55/alzheimers-dataset-4-class-of-images.

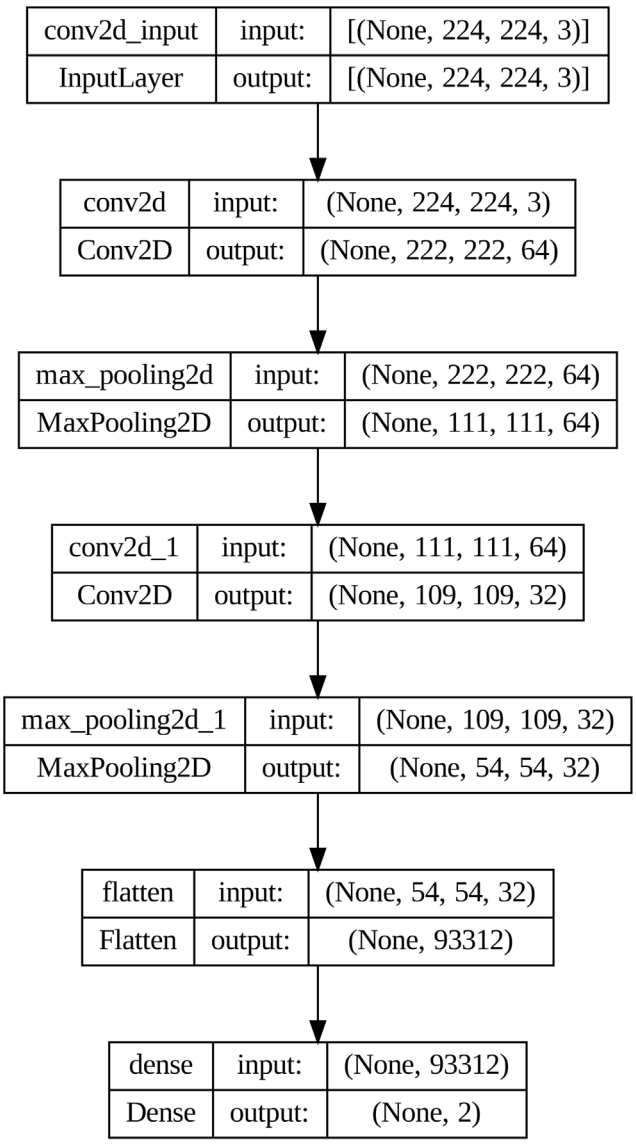

Fig. 7. CNN-SVM-with-Aug model.

Table 1
Total number of images in AD Dataset available in Kaggle.

Class name	Total image
Mild-Demented	896
Moderate-Demented	64
Very-Mild-Demented	2240
Non-Demented	3200

Table 2
Binary classification of AD Dataset.

Class name	Total image
Demented	3200
Non-Demented	3200

Sklearn, were employed to accomplish the programming tasks. The presented models' hyperparameters and standard parameter options, such as the chosen optimizer, loss function, and maximum number of epochs, can be found in Table 3.

Table 3
Hyper Parameters settings for all suggested models..

Algorithm	Parameter
CNNs-without-Aug	Epochs = 100 Batch size = 30 Parameters' number = 2,129,250 Non-trainable parameters = 0 Trainable parameters = 2,129,250 Learning rate = 0.0001 Loss function = binary_Crossentropy Optimizer = Adam
CNNs-with-Aug	Epochs = 100 Batch size = 65 Parameters' number = 6,454,626 Non-trainable parameters = 0 Trainable parameters = 6,454,626 Learning rate = 0.0001 Loss function = binary_Crossentropy Optimizer = Adam
CNNs-LSTM-with-Aug	Epochs = 25 Batch size = 16 Parameters' number = 11,580,858 Non-trainable parameters = 0 Trainable parameters = 11,580,858 Learning rate = 0.0001 Loss function = binary_Crossentropy Optimizer = Adam
CNNs-SVM-with-Aug	Epochs = 20 Batch size = 32 Parameters' number = 206,882 Non-trainable parameters = 0 Trainable parameters = 206,882 Learning rate = 0.0001 Loss function = Squared_hinge Optimizer = Adam
VGG16-SVM-with-Aug	Total number of features by VGG16 = 14,714,688 Non-trainable parameters = 0 Trainable parameters on SVM = 14,714,688 SVM-kernel = Linear

4.3. Evaluation metrics

The assessment of the proposed models reported in this study encompasses many evaluation criteria, such as recall, precision, accuracy, and $F1$-score. The metrics in question are dependent on specific parameters for predictive models, particularly True Positive (TP), True Negative (TN), False Positive (FP), and False Negative (FN). Recall is mathematically represented by Eq. (14), which calculates the true positives' ratio (TP) divided by the totality of true positives (TP) and false negatives (FN). This relationship is expressed mathematically as

It was used to gauge how well the classification outcomes worked. F-measure (F_1) and Accuracy (ACC) (Amigó et al., 2009) are used to gauge how well the classification outcomes worked. $F-$measure gets a single score that balances both the Precision (P) and Recall (R) concerns in one number, as shown in Eq (15).

Let d be the datasets, where $1 \leq i$ and $i \leq n$, and $F = \{D, uD\}$ be the binary classification (where R refers to Demented, uD to non-Demented).

Recall (R) and Precision P can be used to compute the F_1 outcome of the classification issue, as shown in Eq. (15), and Specificity is expressed as in Eq. (17):

$$P_f = \frac{TP_f}{TP_f + FP_f} \tag{13}$$

$$R_f = \frac{TP_f}{TP_f + FN_f} \tag{14}$$

$$F_1 = 2 * \frac{P * R}{P + R} \tag{15}$$

$$Accuracy = \frac{TP + TN}{TP + TN + FP + FN} \tag{16}$$

$$Specificity = \frac{TN}{TN + FP} \tag{17}$$

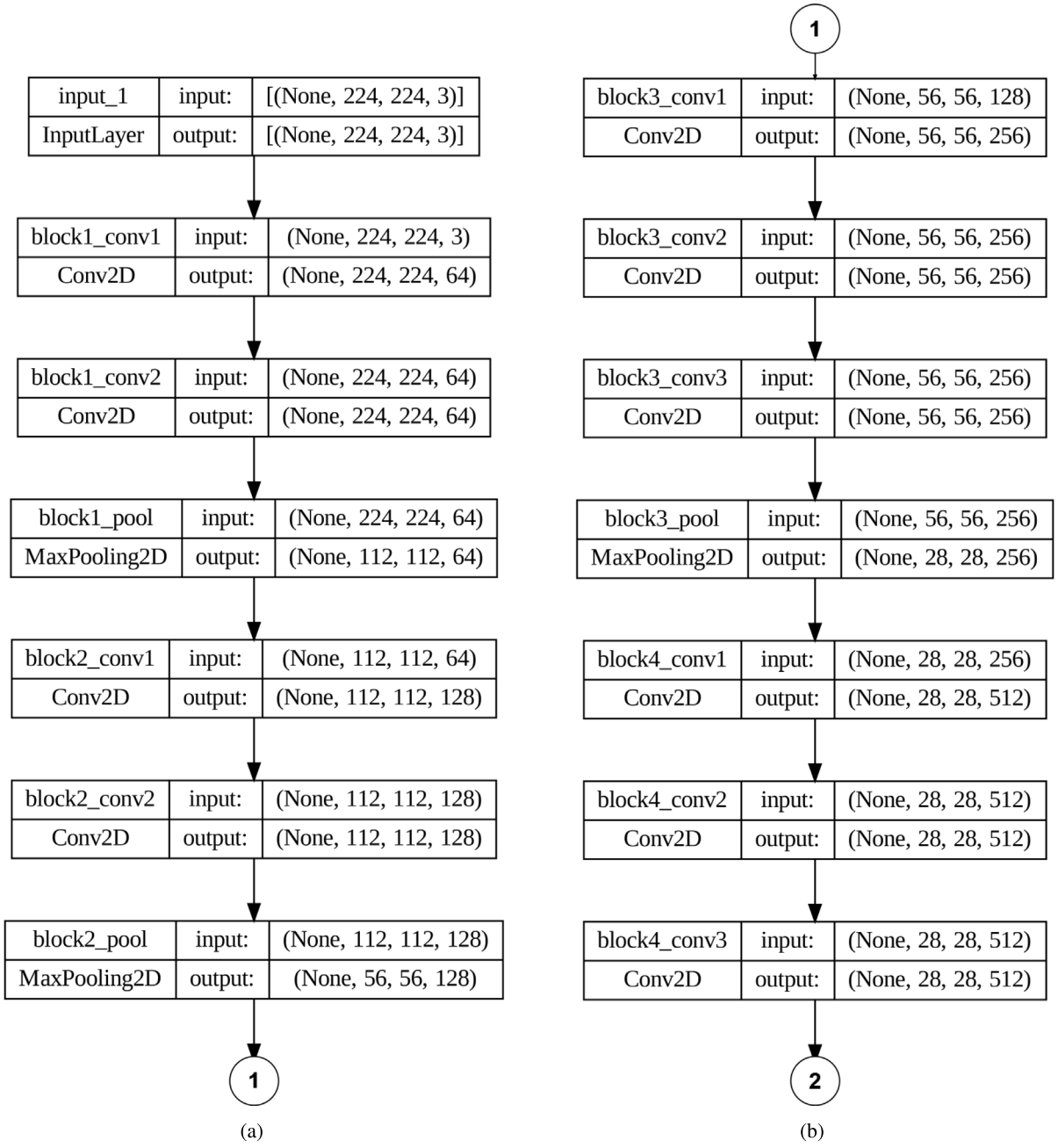

Fig. 8. VGG16 model.

4.4. Comparative analysis

This section aims to estimate the suggested models' performance to address the problem of early AD detection by using binary classification. Different DL models were applied. The goal is to develop a DL model that performs best regarding processing speed and detection accuracy. CNNs is the only model available without-Aug, whereas others are available with-Aug.

4.4.1. The performance results of CNNs-without-Aug model

This Subsection discusses the simulation results of the recommended CNNs-without-Aug. According to Table 3, the recommended CNNs-without-Aug is trained over 100 epochs with a 30 batch size. The suggested CNNs-without-Aug accuracy, loss curves, and confusion matrix are depicted in Fig. 13. For training, the proposed CNNs-without-Aug achieved a 99.69% accuracy. Table 4 provides the suggested CNNs-without-Aug evaluation measures in the testing stage. It scored 99.22%, 100.00%, 95.00%, 100.00%, and 97.39% for accuracy, precision, recall, specificity, and F1-score, respectively.

Table 4
Evaluation metrics of the suggested CNNs-without-Aug.

	Precision	Recall	F1-score
0 (Non-Demented)	99.00	100.00	100.00
1 (Demented)	100.00	95.00	97.00
Macro Avg.	100.00	97.00	98.00
Weighted Avg.	99.00	99.00	99.00
Specificity	100.00		
Accuracy	99.22		

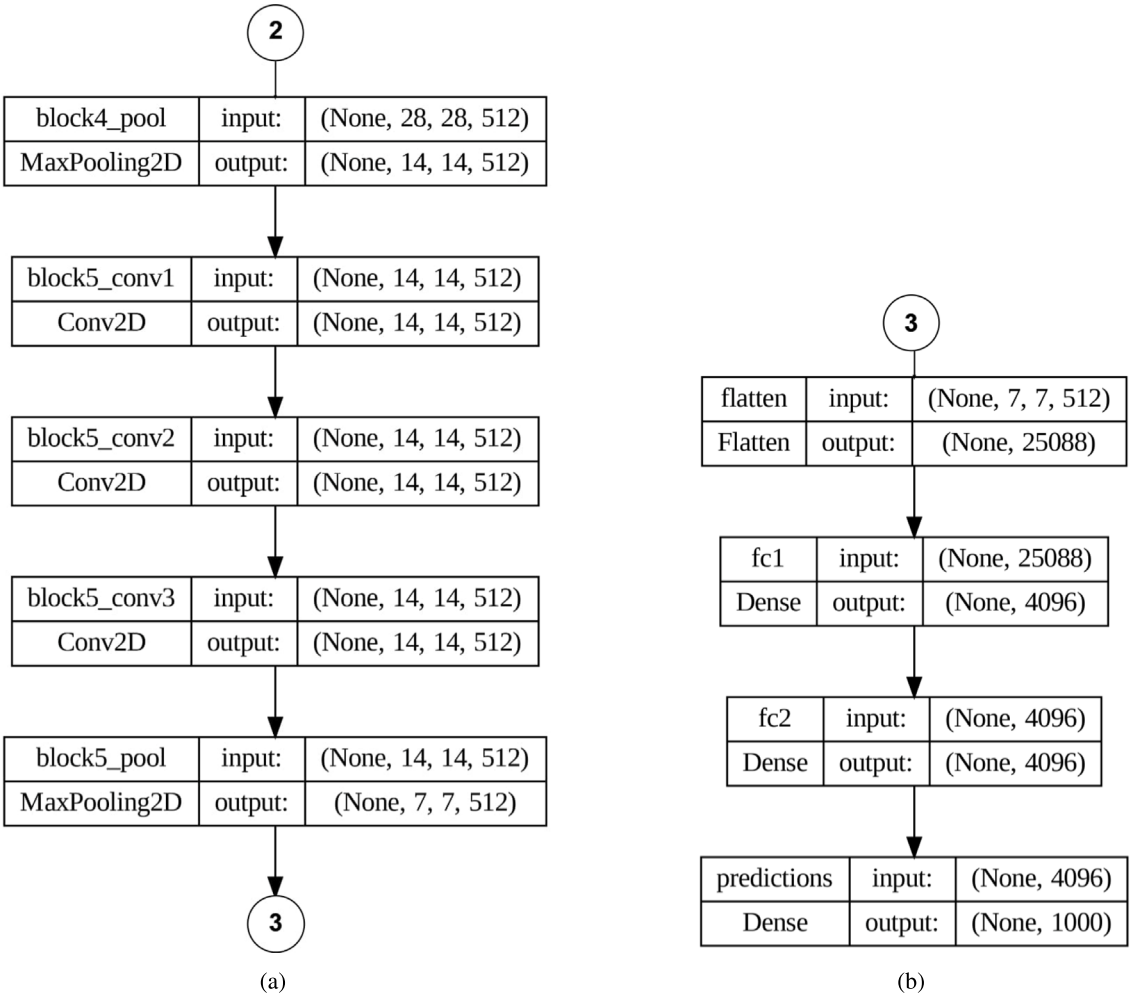

Fig. 9. VGG16 model (Continued).

Table 5
Evaluation metrics of the suggested CNNs-with-Aug.

	Precision	Recall	F1-score
0 (Non-Demented)	100.00	100.00	100.00
1 (Demented)	100.00	97.00	99.00
Macro Avg.	100.00	99.00	99.00
Weighted Avg.	100.00	100.00	100.00
Specificity	100.00		
Accuracy	99.61		

Table 6
Evaluation metrics of the suggested CNNs-LSTM-with-Aug.

	Precision	Recall	F1-score
0 (Non-Demented)	100.00	100.00	100.00
1 (Demented)	100.00	99.00	100.00
Macro Avg.	100.00	100.00	100.00
Weighted Avg.	100.00	100.00	100.00
Specificity	100.00		
Accuracy	99.92		

4.4.2. The performance results of CNNs-with-Aug

This Subsection depicts the experimental results of the recommended CNNs-With-Aug.The recommended CNNs-With-Aug is trained using epochs 100 with a batch size of 65, as shown in Table 3. The suggested CNNs-With-Aug confusion matrix, accuracy, and loss curves are depicted in Fig. 14. For training, the proposed CNNs-With-Aug achieved a 99.85% accuracy. The proposed CNNs-With-Aug evaluation metrics are shown in Table 5 during the testing stage. It obtained 99.61%, 100.00%, 97.39%, 100.00%, and 98.70% for accuracy, precision, recall, specificity, and F1-score, respectively.

4.4.3. The performance results of CNNs-LSTM-with-Aug

This Subsection depicts the experimental results of the suggested hybrid of CNNs-LSTM-with-Aug.The suggested hybrid of CNNs-LSTM-with-Aug is trained using epochs 25 with batch size 16 as shown in Table 3. The suggested hybrid of CNNs-LSTM-with-Aug confusion matrix, accuracy, and loss curves are depicted in Fig. 15. For training, the suggested hybrid of CNNs-LSTM-with-Aug achieved a 100.00% accuracy. The suggested hybrid of CNNs-LSTM-with-Aug evaluation metrics are shown in Table 6 during the testing stage. It obtained 99.92%, 100.00%, 99.50%, 100.00%, and 99.70% for accuracy, precision, recall, specificity, and F1-score, respectively.

4.4.4. The performance results of CNN-SVM-with-Aug

This Subsection discusses the simulation results of the suggested CNN-SVM-With-Aug. Table 3 shows that the suggested CNN-SVM-With-Aug is trained over 20 epochs with a 32 batch size. The suggested CNN-SVM-With-Aug accuracy, loss curves, and confusion matrix are depicted in Fig. 16. For training, The suggested CNN-SVM-With-Aug achieved a 100.00% accuracy. In the testing stage, Table 7 provides

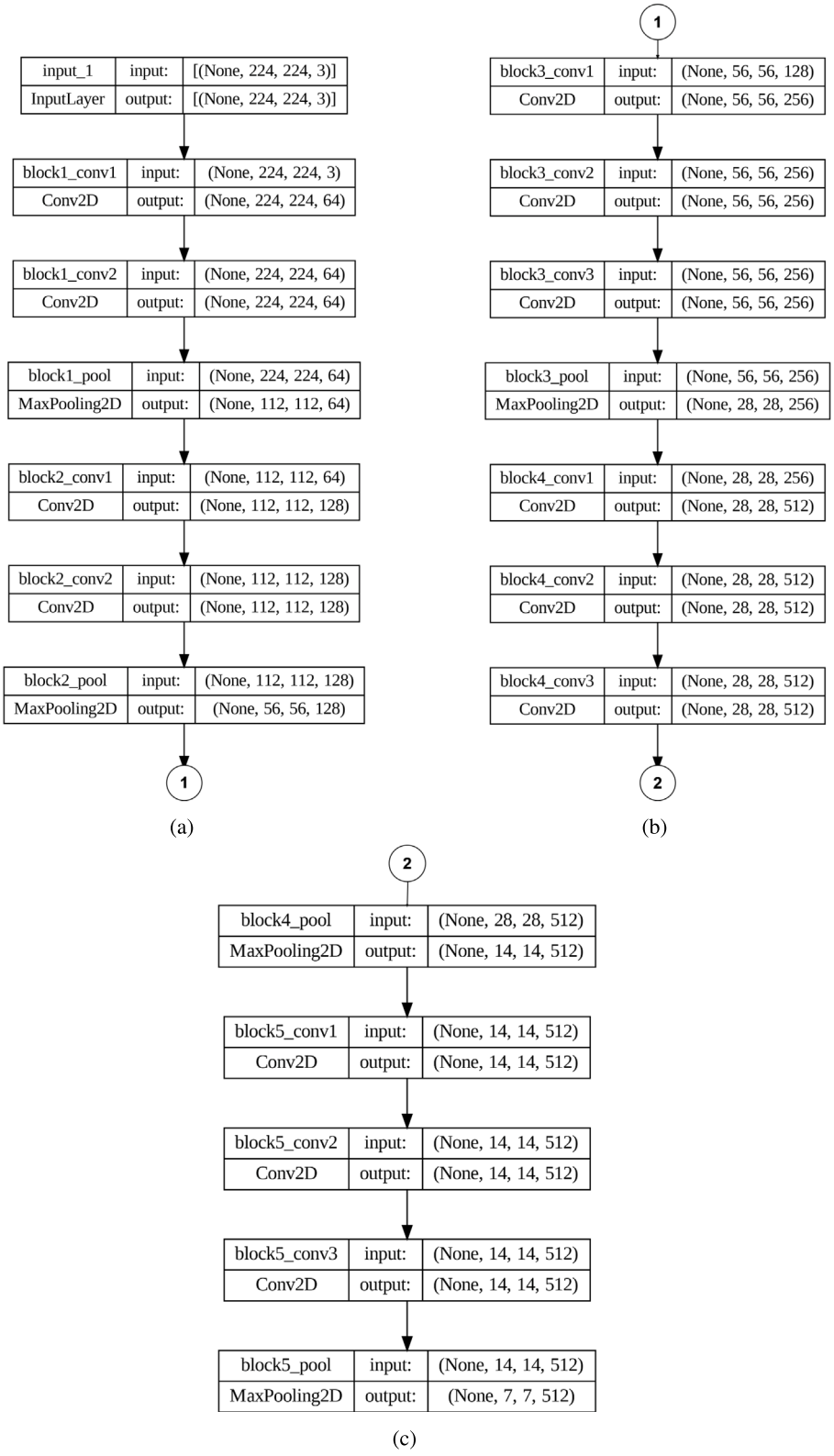

Fig. 10. VGG16 architecture for feature extraction.

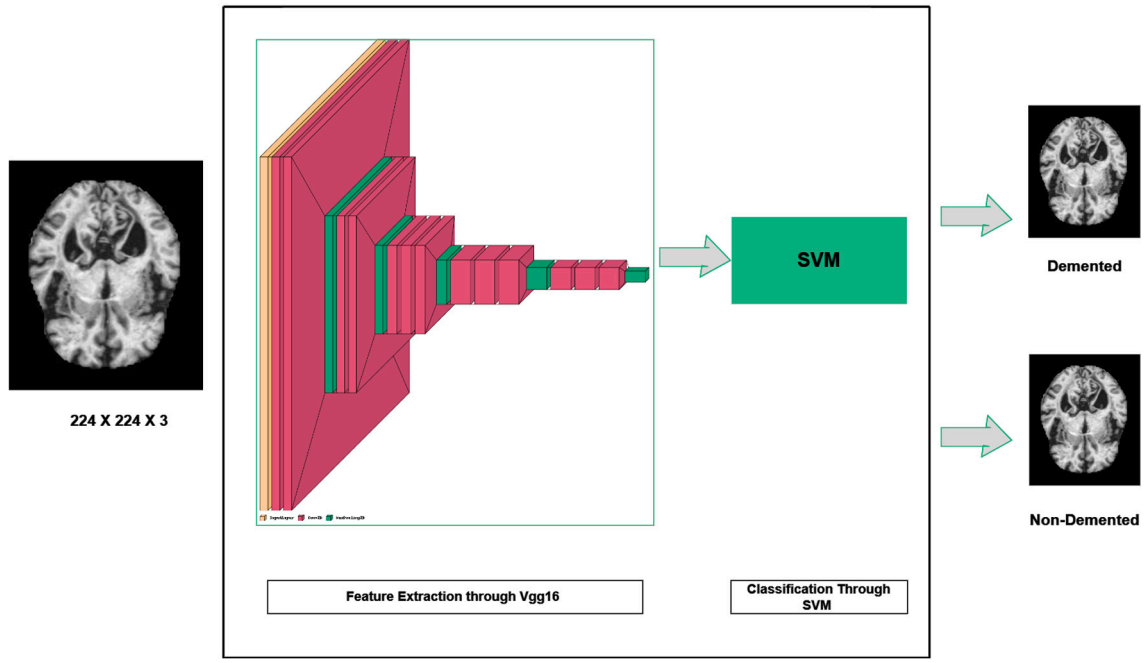

Fig. 11. vgg16-SVM-model-architecture.

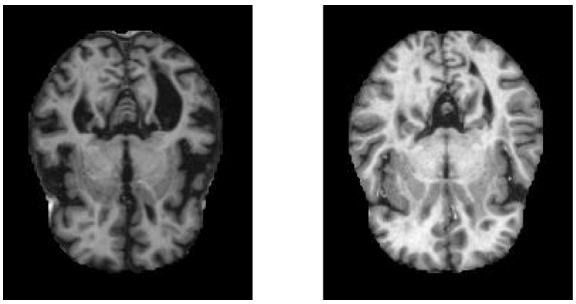

Fig. 12. AD dataset visualization: (a) Demented, (b) Non-Demented.

Table 7
Evaluation metrics of the suggested CNN-SVM-With-Aug.

	Precision	Recall	F1-score
0 (Non-Demented)	99.00	100.00	99.00
1 (Demented)	100.00	94.00	97.00
Macro Avg.	99.00	97.00	98.00
Weighted Avg.	99.00	99.00	99.00
Specificity	100.00		
Accuracy	99.14		

The suggested CNN-SVM-With-Aug achieved evaluation measures. It scored 99.14%, 100.00%, 94.00%, 100.00%, and 97.10% for accuracy, precision, recall, specificity, and F1-score, respectively.

4.4.5. The performance results of Vgg16-SVM with-Aug

This Subsection discusses the simulation results of the suggested Vgg16-SVM-with-Aug model. The suggested Vgg16-SVM-with-Aug is trained according to Table 3. The suggested Vgg16-SVM with-Aug confusion matrix is depicted in Fig. 17. The VGG16-SVM-with-Aug model demonstrated a classification accuracy of 100.00% throughout the training stage. In testing phase, It scored 98.67%, 100.00%, 91.20%, 100.00%, and 95.39% for accuracy, precision, recall, specificity, and F1-score, respectively, as shown in Table 8.

Table 8
Evaluation metrics of the suggested vgg16-SVM-With-Aug.

	Precision	Recall	F1-score
0 (Non-Demented)	98.00	100.00	99.00
1 (Demented)	100.00	91.00	95.00
Macro Avg.	99.00	96.00	97.00
Weighted Avg.	99.00	99.00	99.00
Specificity	100.00		
Accuracy	98.67		

4.5. Comparison with state of art models

Table 9 compares the suggested models to the most binary classification recent models using various datasets. The suggested CNN-LSTM-with-Aug ranked best in all performance metrics, while the proposed CNNs-with-Aug ranked first in precision but second in accuracy, recall, and F1-score.

Because the combination of the CNNs model and the LSTM network can benefit AD early detection using MRI data, the suggested CNNs-LSTM-with-Aug model outperformed the other models in all performance measures. This hybrid architecture can increase the accuracy and performance of the binary classification job by combining the advantages of CNNs and LSTMs.

5. Discussion

This study detailedly evaluated five DL models for AD diagnosis using MRI data, including CNN-without-Aug, CNNs-with-Aug, CNN-LSTM-with-Aug, CNN-SVM-with-Aug, and VGG16-SVM-with-Aug, and the models were assessed on diverse metrics like accuracy, sensitivity, specificity, and precision. The research emphasizes DL's potential in medical imaging and its contributions to future AD detection efforts.

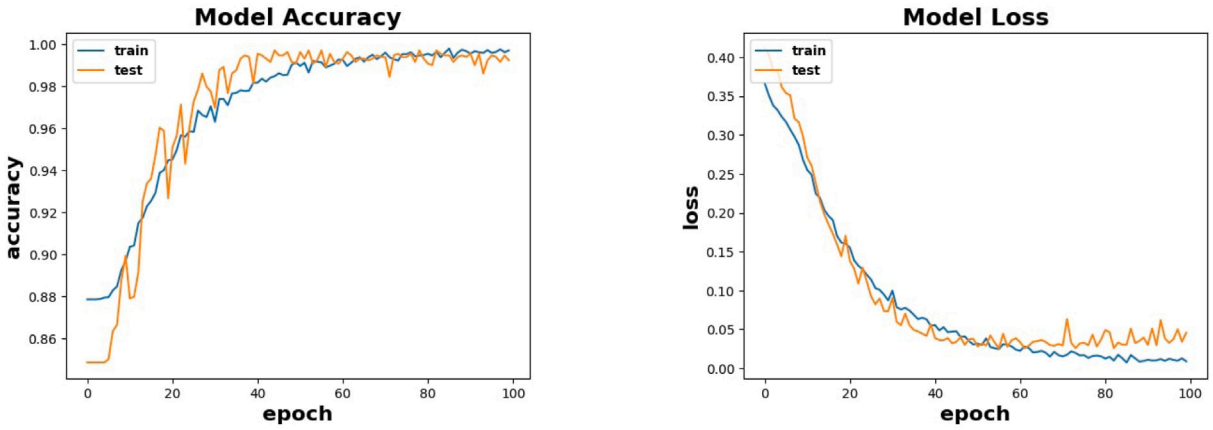

(a) (b)

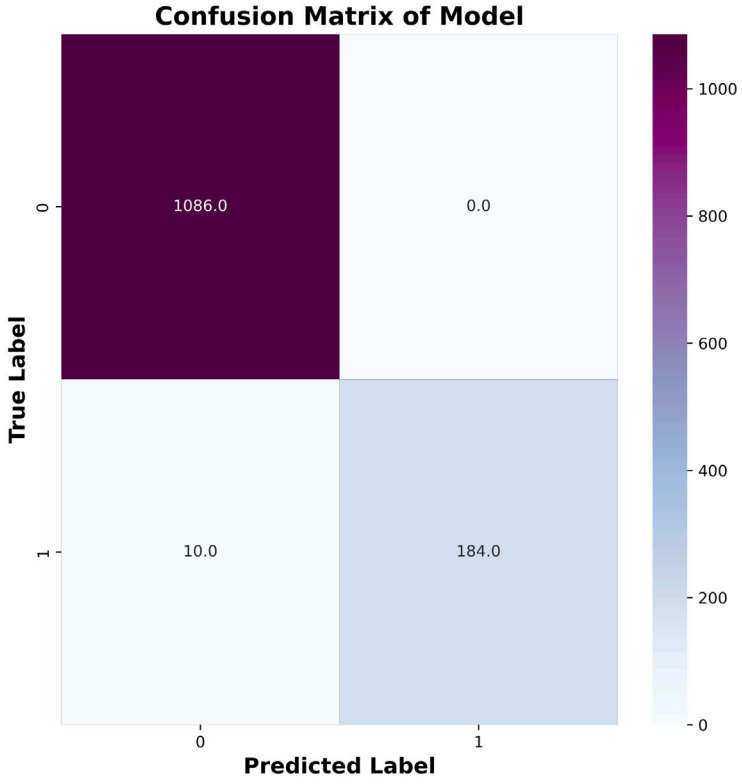

(c)

Fig. 13. Visual results of the suggested CNNs-without-Aug (a) Accuracy curve of the suggested CNNs-without-Aug; (b) Loss curve of the suggested CNNs-without-Aug; and (c) Confusion matrix of the suggested CNNs-without-Aug.

Table 9
Performance analysis of the proposed DL models versus different state-of-the-art DL models.

Model	Author	Database	Accuracy	Precision	Recall	F1-score	Specificity
CNN	Sun et al. (2022)	OASIS	99.68%	–	–	–	–
Hybrid pre-trained models	Sethuraman et al. (2023)	ADNI	96.61%	–	–	–	–
Pre-trained model	Tuvshinjargal and Hwang (2022)	Kaggle	77.40%	77.40%	78.50%	77.90%	–
CNN + LSTM	Balaji et al. (2023)	Kaggle	98.50%	94.80%	98.00%	–	–
Lightweight CNN	Abd (El-Latif et al., 2023)	Kaggle	99.22%	99.22%	99.22%	99.21%	–
3D CNN	Shojaei et al. (2023)	ADNI	96.60%	–	–	–	–
CNN-LSTM-With-AUG			**99.92%**	**100.00%**	**99.50%**	**99.70%**	**100.00%**
CNNs-with-Aug	The proposed models	Kaggle	99.61%	**100.00%**	97.39%	98.70%	**100.00%**
CNN-Without-Aug			99.22%	**100.00%**	95.00%	97.39%	**100.00%**
CNN-SVM-with-Aug			99.14%	**100.00%**	94.00%	97.10%	**100.00%**
Vgg16-SVM-With-Aug			98.67%	**100.00%**	91.20%	95.39%	**100.00%**

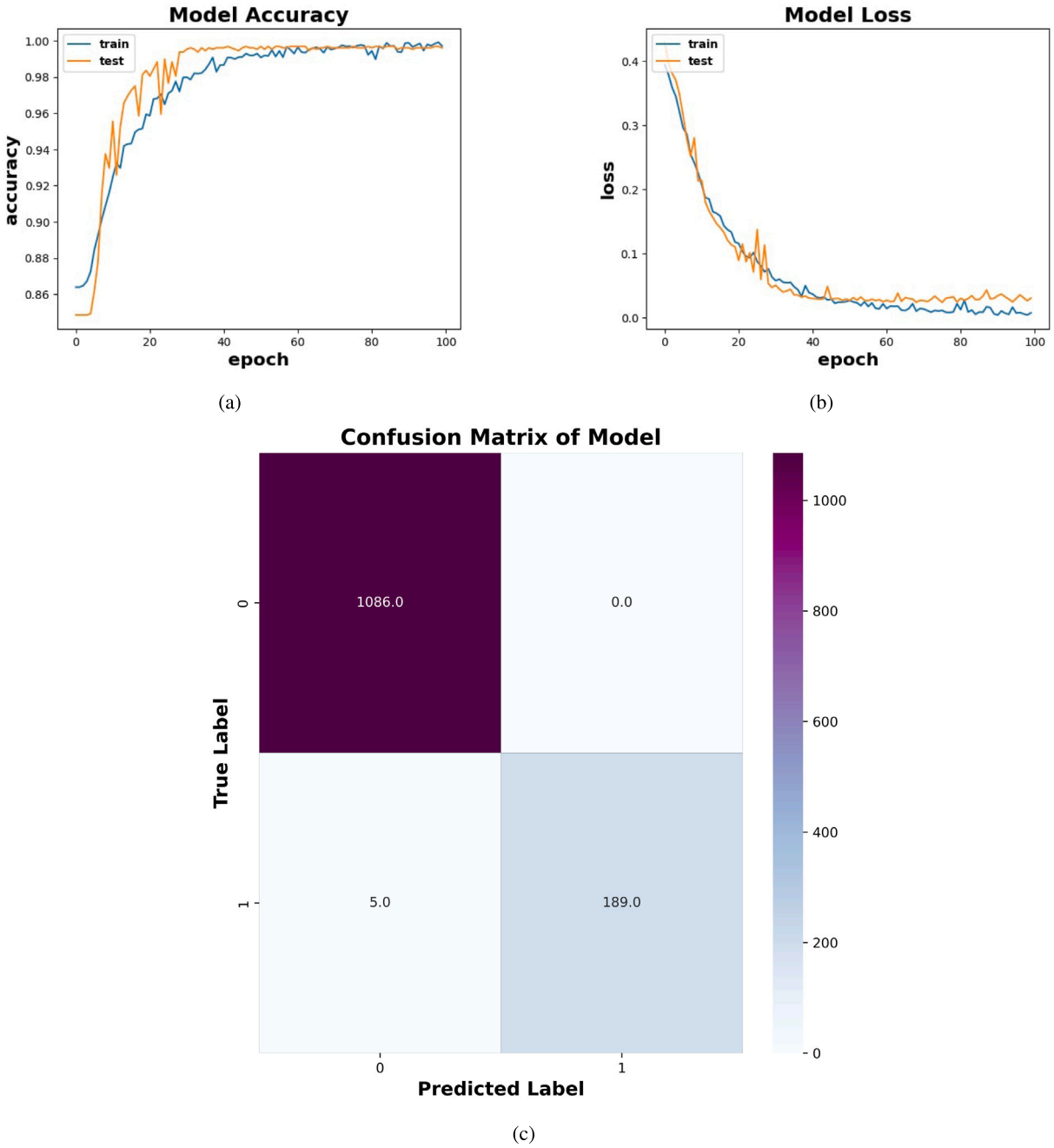

Fig. 14. Visual results of the suggested CNNs-With-Aug (a) Accuracy curve of the suggested CNNs-With-Aug; (b) Loss curve of the suggested CNNs-With-Aug; and (c) Confusion matrix of the suggested CNNs-With-Aug.

Table 10 presents a comparison between the suggested models using the ADs dataset as a basis for evaluating the performance of the suggested models. Additionally, it provides the processing time, encompassing both the training and testing durations. The presence of trade-offs between detection precision and processing time is apparent. The CNNs-without-Aug attained a classification accuracy of 99.22%. This model's training and testing durations were recorded as 224 s and 4 ms, respectively. This characteristic renders it a viable option for real-time applications. In contrast, the CNN model using data augmentation (CNNs-with-Aug) attained a precision of 99.61%. This model's training and testing durations were 538 s and 7 ms, respectively. Furthermore, the CNNs-LSTM-with-Aug had a commendable accuracy rate of 99.92%. This model's training and testing durations were recorded as 360 s and 9 ms, respectively. In a similar vein, the model known as CNNs-SVM-with-Aug demonstrated an accuracy rate of 99.14%. This model's training and testing durations were recorded as 171 s and 11 ms, respectively. Also, In a similar vein, the model known as vgg16-SVM-with-Aug demonstrated an accuracy rate of 98.67%. This model's training and testing durations were recorded as 210 s and 50 ms,

Considering the outcomes that were attained, it could be argued that the **CNNs-without-Aug model** is the optimal choice for promptly identifying AD in real-time scenarios as it is the lowest time in Predicting time. Additionally, It is first in precision and specificity. It is also the third in accuracy, Recall, and F1-score. **The Suggested CNNs-LSTM-with-Aug** has superior accuracy, precision, recall, and F1-score for detection, and it is also third in predicting time. **The suggested CNNs-with-Aug** is the first in precision and specificity, the second in accuracy, recall, F1-score, and predicting time. **The suggested CNN-SVM–with-Aug** is the first in precision and specificity; it is also the fourth in accuracy, F1-score, Recall, and predicting time.

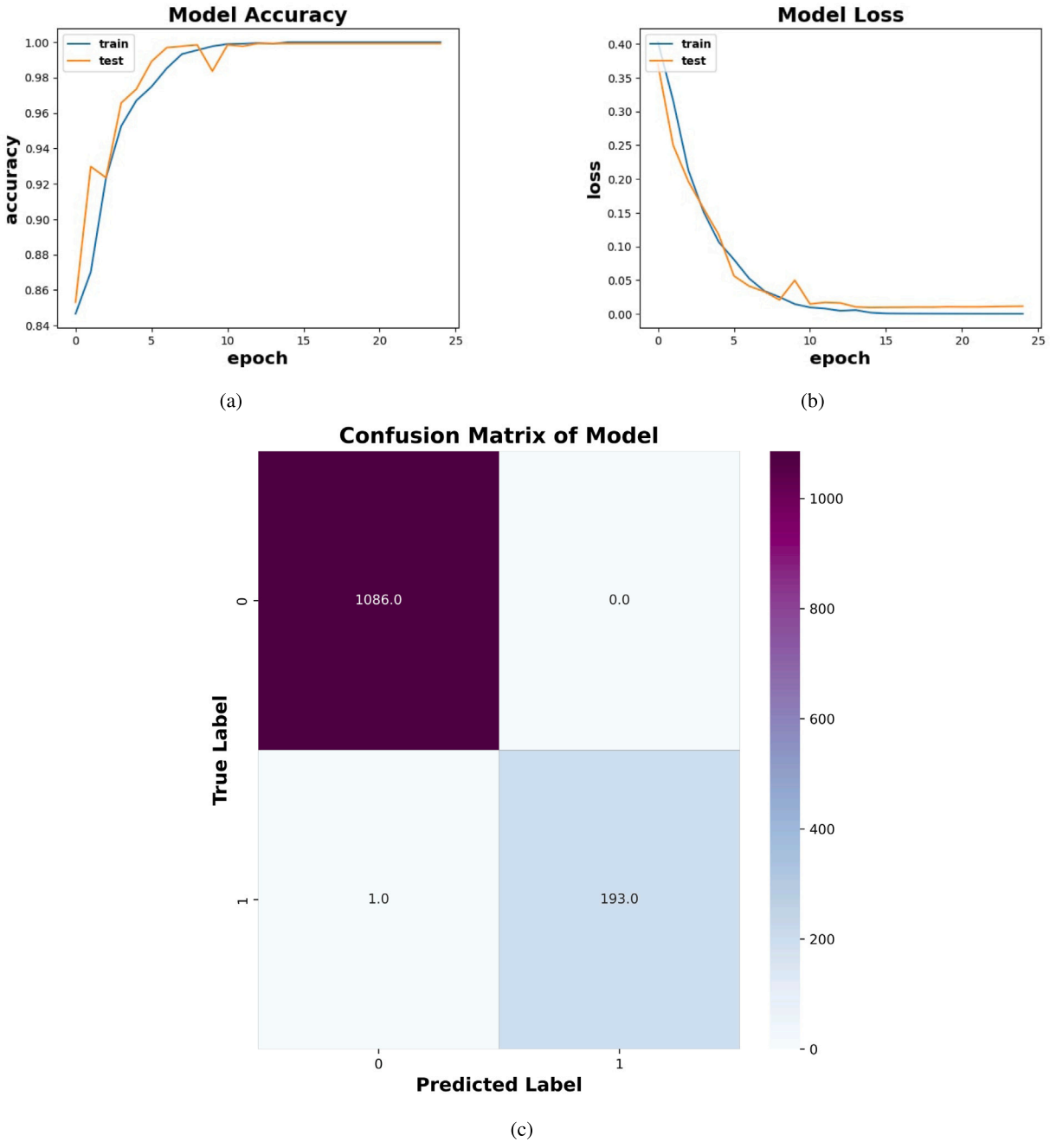

Fig. 15. Visual results of the suggested hybrid of CNNs-LSTM-with-Aug (a) Accuracy curve of the suggested hybrid of CNNs-LSTM-with-Aug; (b) Loss curve of the suggested hybrid of CNNs-LSTM-with-Aug; and (c) Confusion matrix of the suggested hybrid of CNNs-LSTM-with-Aug.

Table 10
Comparison between the proposed DL models using specific evaluation metrics.

Model	Accuracy	Precision	Recall	F1-score	Specificity	Training time	Testing time
CNN-LSTM-With-AUG	99.92%	100.00%	99.50%	99.70%	100.00%	360 s	9 ms
CNNs-with-Aug	99.61%	100.00%	97.39%	98.70%	100.00%	538 s	7 ms
CNN-without-AUG	99.22%	100.00%	95.00%	97.39%	100.00%	224 s	4 ms
CNN-SVM-with-Aug	99.14%	100.00%	94.00%	97.10%	100.00%	171 s	11 ms
Vgg16-SVM with-Aug	98.67%	100.00%	91.20%	95.39%	100.00%	210 s	50 s

The suggested Vgg16-SVM-with-Aug is the last in all performance measures.

Among the models, CNNs-LSTM-with-Aug emerged as superior in swiftly detecting AD, offering high accuracy, precision, recall, and F1-score. However, the CNNs-without-Aug model is favored for immediate AD identification in real-time scenarios. LSTMs, with their capacity to identify temporal dependencies in consecutive data, are advantageous in AD categorization, addressing overfitting risks associated with CNNs, especially in limited datasets. DL is crucial for early AD detection for several reasons, including enhanced accuracy, early intervention, objective assessment, scalability, efficiency, support in drug development, personalized treatment plans, cost savings, and advancement

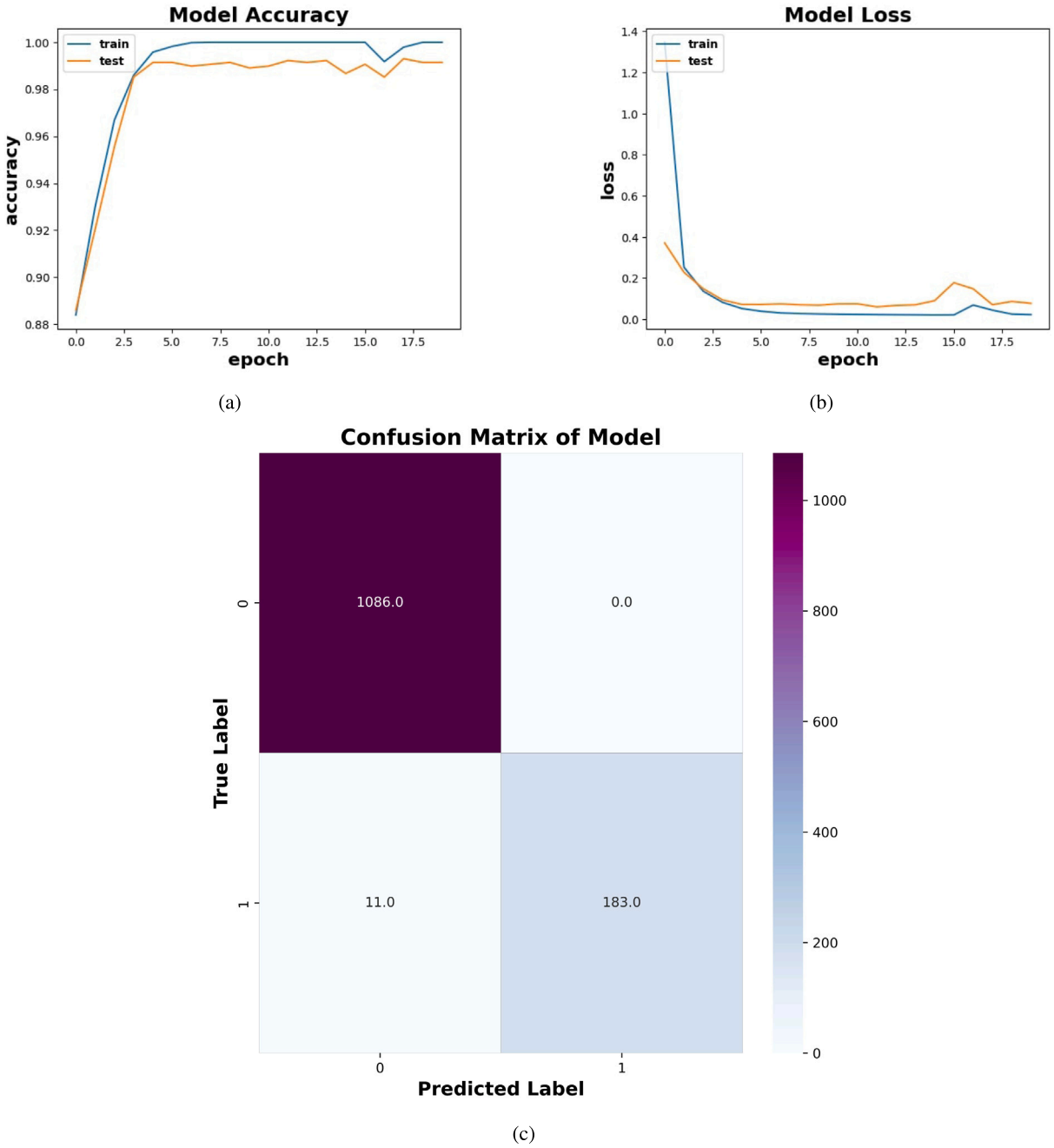

Fig. 16. Visual results of the suggested hybrid of CNN-SVM-With-Aug (a) Accuracy curve of the suggested hybrid of CNN-SVM-With-Aug; (b) Loss curve of the suggested hybrid of CNN-SVM-With-Aug; and (c) Confusion matrix of the suggested hybrid of CNN-SVM-With-Aug.

in research. Its precision, ability to improve patient outcomes and contributions to healthcare and research make DL an essential tool in combating AD. The following points illustrate some of the advantages of relying on the CNN-LSTM architecture for AD classification:

- **Hierarchical feature extraction**: CNNs are ideal for capturing spatial patterns and hierarchical features from images. CNNs may extract relevant features from the raw MRI data and highlight textures, edges, and local patterns that are indicative of various brain structures or abnormalities associated with AD.
- **Temporal information handling**: Sequential data's temporal dependencies can be captured using LSTMs. The sequential nature of MRI images obtained over time can be utilized by LSTMs in the context of AD classification. By studying the sequence of images and their associated metadata, if accessible, LSTMs may track the disease progression.
- **Spatial–temporal patterns incorporation**: The spatial features extracted by CNNs and the temporal dependencies captured by LSTMs can be combined using the hybrid architecture. This enables the model to represent both short-term and long-term alterations in the brain's structure that might be suggestive of AD progression.
- **Contextual understanding improvement**: AD is a progressive neurodegenerative illness that gradually affects brain structures. By combining CNNs and LSTMs, the model can understand the context of changes in brain scans and how they evolve during the disease's progression, leading to more accurate classification.
- **Overfitting reduction**: LSTMs can assist the model in becoming more regular and less overfitting. CNNs tend to have a huge

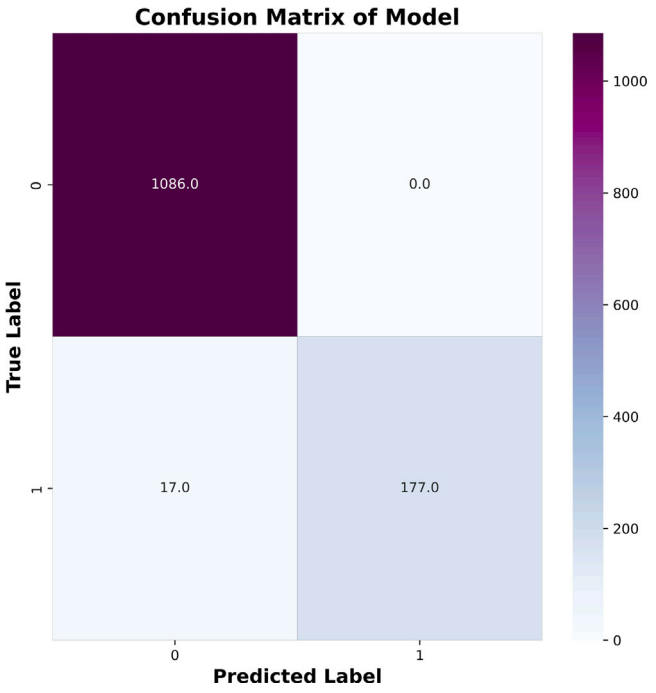

Fig. 17. Confusion matrix of VGG16-SVM-with-Aug model.

number of parameters, which increases the risk of overfitting, especially when the dataset is limited. The LSTMs' ability to capture temporal relationships can aid in preventing the model from memorizing the training data.

- **Interpretable features**: The CNN-LSTM architecture can provide interpretable features, where the CNN component can highlight pertinent image regions, and the LSTM component can show how the patterns in these regions evolve over time. This interpretability can be crucial in the medical domain.
- **Adaptable to varying data sequences**: The hybrid architecture may adapt to varying numbers of MRI images for various patients, making it a more flexible method.
- **Early detection possibility**: The CNN-LSTM model may have the potential to detect subtle changes in brain structure that could be an early sign of AD by leveraging both spatial and temporal information, enabling timely intervention.

6. Conclusion

Prominent clinical manifestations, including notable deficits in memory, cognitive impairment, and disorientation, may serve as indicative markers of neuronal degradation, representing an early and prevalent indication of AD. The symptoms above gradually deteriorate over time, negatively affecting an individual's overall well-being. Although a cure for AD remains elusive, the provision of timely and efficient care has the potential to enhance the quality of life and decelerate the condition's advancement. MRI scans are a highly valuable dataset utilized for detecting AD. In the area of analysis of medical images, DL models are commonly employed. The primary objective of the presented work was to examine and evaluate two distinct approaches and five DL architectures in the context of AD identification. The utilization of the CNN architecture is observed in scenarios when data augmentation is not implemented (CNN-without-Aug). In contrast, the utilization of data augmentation entails the implementation of four primary architectural approaches: CNNs-with-Aug, CNNs-LSTM-with-Aug, CNNs-SVM-with-Aug, and transfer learning, including VGG16-SVM-with-Aug. One pertinent inquiry that emerges is the reason for the superior performance of CNNs-LSTM-with-Aug compared to alternative architectures, including other models like CNNs-with-Aug.

As compared to other models, the suggested CNNs-LSTM-with-Aug architecture performed better overall, and it is presently recommended for the diagnosis of AD. With a negligible loss of 0.0160, the suggested CNNs-LSTM-with-Aug architecture achieved 100.00% training accuracy and 99.92% testing accuracy. These findings show that it may effectively categorize AD cases accurately by incorporating data augmentation techniques. With the help of LSTM layers, the suggested CNN-LSTM-with-Aug was able to recognize temporal relationships in image sequences, which made it appropriate for evaluating sequential data such as movies. Its 100.00% precision means that every positive instance was accurately recognized; its 100.00% specificity means that every true negative was correctly identified and no false positives were created; and its 99.50% recall indicates that the majority of positive cases were successfully discovered. The computational efficiency of the suggested CNNs-LSTM-with-Aug architecture is confirmed by the F1-score of 99.70%, which indicates a strong balance between precision and recall. It obtains its excellent performance in just 25 epochs with a batch size of 16. In contrast, the CNN-with-Aug architecture that was suggested used data augmentation methods to enhance the training set, which resulted in better generalization skills. It accurately anticipated every positive event with 100.00% precision. With a recall of 97.39%, it demonstrates its effectiveness in recognizing positive instances, and its specificity of 100.00% means that it accurately detected all true negatives. Its balanced performance has been further validated with an F1-score of 98.70%. However, in comparison with the CNN-LSTM-Aug model, it took longer to train with a batch size of 65 and needed 100 epochs to achieve its high accuracy.

Ultimately, It can be said that these DL models represent a significant advancement in the early diagnosis of AD by image data analysis, which may have a favorable effect on the medical field. The proposed DL models might develop into useful tools to help medical researchers and healthcare practitioners classify AD with more improvement in validation, refinement, and interpretability. Therefore, to obtain more reliable findings for Alzheimer's detection in the future, recently built DL models and pre-trained deep architectures may be used. Using DL algorithms, a few additional issues that affect people and their health will also be concentrated on.

Declaration of competing interest

The authors declare that they have no known competing financial interests or personal relationships that could have appeared to influence the work reported in this paper.

Acknowledgments

The authors extend their sincere thanks to the Deanship of Scientific Research, Vice Presidency for Graduate Studies and Scientific Research, King Faisal University, Saudi Arabia for their generous financial support, which was crucial for the research project (GRANT 5,608).

References

Ahmed, S., Choi, K.Y., Lee, J.J., Kim, B.C., Kwon, G.-R., Lee, K.H., Jung, H.Y., 2019. Ensembles of patch-based classifiers for diagnosis of Alzheimer diseases. IEEE Access 7, 73373–73383.

Ahmed, I.A., Senan, E.M., Shatnawi, H.S.A., Alkhraisha, Z.M., Al-Azzam, M.M.A., 2023. Multi-techniques for analyzing X-ray images for early detection and differentiation of pneumonia and tuberculosis based on hybrid features. Diagnostics 13 (4), 814.

Ajagbe, S.A., Amuda, K.A., Oladipupo, M.A., Oluwaseyi, F.A., Okesola, K.I., 2021. Multi-classification of Alzheimer disease on magnetic resonance images (MRI) using deep convolutional neural network (DCNN) approaches. Int. J. Adv. Comput. Res. 11 (53), 51.

Alnaim, A.K., Alwakeel, A.M., 2023. Machine-learning-based IoT–edge computing healthcare solutions. Electronics 12 (4), 1027.

Alorf, A., Khan, M.U.G., 2022. Multi-label classification of Alzheimer's disease stages from resting-state fMRI-based correlation connectivity data and deep learning. Comput. Biol. Med. 151, 106240.

Amigó, E., Gonzalo, J., Artiles, J., Verdejo, F., 2009. A comparison of extrinsic clustering evaluation metrics based on formal constraints. Inf. Retr. 12, 461–486.
Ávila-Jiménez, J., Cantón-Habas, V., del Pilar Carrera-González, M., Rich-Ruiz, M., Ventura, S., 2023. A deep learning model for Alzheimer's disease diagnosis based on patient clinical records. Comput. Biol. Med. 107814.
Bae, J.B., Lee, S., Jung, W., Park, S., Kim, W., Oh, H., Han, J.W., Kim, G.E., Kim, J.S., Kim, J.H., et al., 2020. Identification of Alzheimer's disease using a convolutional neural network model based on T1-weighted magnetic resonance imaging. Sci. Rep. 10 (1), 22252.
Balaji, P., Chaurasia, M.A., Bilfaqih, S.M., Muniasamy, A., Alsid, L.E.G., 2023. Hybridized deep learning approach for detecting Alzheimer's disease. Biomedicines 11 (1), 149.
Battineni, G., Hossain, M.A., Chintalapudi, N., Traini, E., Dhulipalla, V.R., Ramasamy, M., Amenta, F., 2021. Improved Alzheimer's disease detection by MRI using multimodal machine learning algorithms. Diagnostics 11 (11), 2103.
Bhadra, S., Kumar, C.J., 2022. An insight into diagnosis of depression using machine learning techniques: a systematic review. Curr. Med. Res. Opin. 38 (5), 749–771.
Biagetti, G., Crippa, P., Falaschetti, L., Luzzi, S., Turchetti, C., 2021. Classification of Alzheimer's disease from EEG signal using robust-PCA feature extraction. Procedia Comput. Sci. 192, 3114–3122.
Cheung, C.Y., Ran, A.R., Wang, S., Chan, V.T., Sham, K., Hilal, S., Venketasubramanian, N., Cheng, C.-Y., Sabanayagam, C., Tham, Y.C., et al., 2022. A deep learning model for detection of Alzheimer's disease based on retinal photographs: a retrospective, multicentre case-control study. Lancet Digit. Health 4 (11), e806–e815.
Desai, P., Pujari, J., Sujatha, C., Kamble, A., Kambli, A., 2021. Hybrid approach for content-based image retrieval using VGG16 layered architecture and SVM: an application of deep learning. SN Comput. Sci. 2, 1–9.
Diogo, V.S., Ferreira, H.A., Prata, D., Initiative, A.D.N., 2022. Early diagnosis of Alzheimer's disease using machine learning: a multi-diagnostic, generalizable approach. Alzheimer's Res. Ther. 14 (1), 107.
El-Latif, A.A.A., Chelloug, S.A., Alabdulhafith, M., Hammad, M., 2023. Accurate detection of Alzheimer's disease using lightweight deep learning model on MRI data. Diagnostics 13 (7), 1216.
Farina, F., Emek-Savaş, D., Rueda-Delgado, L., Boyle, R., Kiiski, H., Yener, G., Whelan, R., 2020. A comparison of resting state EEG and structural MRI for classifying Alzheimer's disease and mild cognitive impairment. Neuroimage 215, 116795.
Fathi, S., Ahmadi, M., Dehnad, A., 2022. Early diagnosis of Alzheimer's disease based on deep learning: A systematic review. Comput. Biol. Med. 146, 105634.
Helaly, H.A., Badawy, M., Haikal, A.Y., 2021. Deep learning approach for early detection of Alzheimer's disease. Cogn. Comput. 1–17.
Islam, J., Zhang, Y., 2018. Brain MRI analysis for Alzheimer's disease diagnosis using an ensemble system of deep convolutional neural networks. Brain Inform. 5, 1–14.
Jindal, S., Sharma, A., Joshi, A., Gupta, M., 2021. Artificial intelligence fuelling the health care. In: Mobile Radio Communications and 5G Networks: Proceedings of MRCN 2020. Springer, hhh, pp. 501–507.
Jo, T., Nho, K., Saykin, A.J., 2019. Deep learning in Alzheimer's disease: diagnostic classification and prognostic prediction using neuroimaging data. Front. Aging Neurosci. 11, 220.
Khojaste-Sarakhsi, M., Haghighi, S.S., Ghomi, S.F., Marchiori, E., 2022. Deep learning for Alzheimer's disease diagnosis: A survey. Artif. Intell. Med. 130, 102332.
Kishore, N., Goel, N., 2023. Deep learning based diagnosis of Alzheimer's disease using FDG-PET images. Neurosci. Lett. 817, 137530.
Lakhan, A., Grønli, T.-M., Muhammad, G., Tiwari, P., 2023. EDCNNS: Federated learning enabled evolutionary deep convolutional neural network for Alzheimer disease detection. Appl. Soft Comput. 147, 110804.
Lee, G., Nho, K., Kang, B., Sohn, K.-A., Kim, D., 2019. Predicting Alzheimer's disease progression using multi-modal deep learning approach. Sci. Rep. 9 (1), 1952.
Leela, M., Helenprabha, K., Sharmila, L., 2023. Prediction and classification of Alzheimer Disease categories using integrated deep transfer learning approach. Meas.: Sens. 27, 100749.
Nagarajan, S.M., Devarajan, G.G., Mohammed, A.S., Ramana, T., Ghosh, U., 2022. Intelligent task scheduling approach for IoT integrated healthcare cyber physical systems. IEEE Trans. Netw. Sci. Eng. 10, 2429–2438.
Nagarajan, S.M., Muthukumaran, V., Murugesan, R., Joseph, R.B., Munirathanam, M., 2021. Feature selection model for healthcare analysis and classification using classifier ensemble technique. Int. J. Syst. Assur. Eng. Manag. 10 (34), 1–12.
Nalini, T., Rama, A., 2022. Impact of temperature condition in crop disease analyzing using machine learning algorithm. Meas.: Sens. 24, 100408.
Odusami, M., Maskeliūnas, R., Damaševičius, R., 2022. An intelligent system for early recognition of Alzheimer's disease using neuroimaging. Sensors 22 (3), 740.
Odusami, M., Maskeliūnas, R., Damaševičius, R., Misra, S., 2023. Explainable deep-learning-based diagnosis of Alzheimer's disease using multimodal input fusion of PET and MRI images. J. Med. Biol. Eng. 1–12.
Ortiz, A., Munilla, J., Gorriz, J.M., Ramirez, J., 2016. Ensembles of deep learning architectures for the early diagnosis of the Alzheimer's disease. Int. J. Neural Syst. 26 (07), 1650025.
Pan, X., Phan, T.-L., Adel, M., Fossati, C., Gaidon, T., Wojak, J., Guedj, E., 2020a. Multi-view separable pyramid network for AD prediction at MCI stage by 18 F-FDG brain PET imaging. IEEE Trans. Med. Imaging 40 (1), 81–92.
Pan, D., Zeng, A., Jia, L., Huang, Y., Frizzell, T., Song, X., 2020b. Early detection of Alzheimer's disease using magnetic resonance imaging: a novel approach combining convolutional neural networks and ensemble learning. Front. Neurosci. 14, 259.
Prasath, T., Sumathi, V., 2024. Pipelined deep learning architecture for the detection of Alzheimer's disease. Biomed. Signal Process. Control 87, 105442.
Raju, M., Gopi, V.P., Anitha, V., 2021. Multi-class classification of Alzheimer's Disease using 3DCNN features and multilayer perceptron. In: 2021 Sixth International Conference on Wireless Communications, Signal Processing and Networking. WiSPNET, IEEE, www, pp. 368–373.
Rohini, G., 2021. Everything you need to know about VGG16. Medium Available online: https://medium.com/@mygreatlearning/everything-you-need-to-know-about-vgg16-7315defb5918.
Rolls, E.T., Huang, C.-C., Lin, C.-P., Feng, J., Joliot, M., 2020. Automated anatomical labelling atlas 3. Neuroimage 206, 116189.
Saied, I.M., Arslan, T., Chandran, S., 2021. Classification of Alzheimer's disease using RF signals and machine learning. IEEE J. Electromagn. RF Microw. Med. Biol. 6 (1), 77–85.
Saini, K., Marriwala, N., 2022. Deep learning-based face mask detecting system: an initiative against COVID-19. In: Emergent Converging Technologies and Biomedical Systems: Select Proceedings of ETBS 2021. Springer, oooo, pp. 729–742.
Saleem, T.J., Zahra, S.R., Wu, F., Alwakeel, A., Alwakeel, M., Jeribi, F., Hijji, M., 2022. Deep learning-based diagnosis of Alzheimer's disease. J. Pers. Med. 12 (5), 815.
Sarraf, S., Tofighi, G., 2016. Deep learning-based pipeline to recognize Alzheimer's disease using fMRI data. In: 2016 Future Technologies Conference. FTC, IEEE, pp. 816–820.
Sethuraman, S.K., Malaiyappan, N., Ramalingam, R., Basheer, S., Rashid, M., Ahmad, N., 2023. Predicting Alzheimer's disease using deep neuro-functional networks with resting-state fMRI. Electronics 12 (4), 1031.
Sharma, S., Guleria, K., 2022. Deep learning models for image classification: comparison and applications. In: 2022 2nd International Conference on Advance Computing and Innovative Technologies in Engineering. ICACITE, IEEE, ggg, pp. 1733–1738.
Shi, Y., Zeng, W., Deng, J., Nie, W., Zhang, Y., 2020. The identification of Alzheimer's disease using functional connectivity between activity voxels in resting-state fMRI data. IEEE J. Transl. Eng. Health Med. 8, 1–11.
Shojaei, S., Abadeh, M.S., Momeni, Z., 2023. An evolutionary explainable deep learning approach for Alzheimer's MRI classification. Expert Syst. Appl. 220, 119709.
Shukla, A., Tiwari, R., Tiwari, S., 2023. Review on alzheimer disease detection methods: Automatic pipelines and machine learning techniques. Sci 5 (1), 13.
Smagulova, K., James, A.P., 2019. A survey on LSTM memristive neural network architectures and applications. Eur. Phys. J. Spec. Top. 228 (10), 2313–2324.
Sosa-Ortiz, A.L., Acosta-Castillo, I., Prince, M.J., 2012. Epidemiology of dementias and Alzheimer's disease. Arch. Med. Res. 43 (8), 600–608.
Staudemeyer, R.C., Morris, E.R., 2019. Understanding LSTM–a tutorial into long short-term memory recurrent neural networks. arXiv preprint arXiv:1909.09586.
Subramoniam, M., Aparna, T., Anurenjan, P., Sreeni, K., 2022. Deep learning-based prediction of Alzheimer's disease from magnetic resonance images. In: Intelligent Vision in Healthcare. Springer, pp. 145–151.
Sun, J., Gong, Y., Liu, M., Liang, C., Zhao, Y., 2022. A uniform allowance matching method for point cloud based on the edge extraction under de-shaping center. Alex. Eng. J. 61 (12), 12965–12976.
Trivedi, N.K., Anand, A., Lilhore, U.K., Guleria, K., 2022. Deep learning applications on edge computing. In: Machine Learning for Edge Computing, first ed. CRC Press, pp. 143–168.
Tun, N.L., Gavrilov, A., Tun, N.M., Aung, H., et al., 2021. Remote sensing data classification using a hybrid pre-trained VGG16 CNN-SVM classifier. In: 2021 IEEE Conference of Russian Young Researchers in Electrical and Electronic Engineering. ElConRus, IEEE, pp. 2171–2175.
Tuvshinjargal, B., Hwang, H., 2022. VGG-C transform model with batch normalization to predict Alzheimer's disease through MRI dataset. Electronics 11 (16), 2601.
van Veen, R., Meles, S.K., Renken, R.J., Reesink, F.E., Oertel, W.H., Janzen, A., De Vries, G.-J., Leenders, K.L., Biehl, M., 2022. FDG-PET combined with learning vector quantization allows classification of neurodegenerative diseases and reveals the trajectory of idiopathic REM sleep behavior disorder. Comput. Methods Programs Biomed. 225, 107042.
Vogt, A.-C.S., Jennings, G.T., Mohsen, M.O., Vogel, M., Bachmann, M.F., 2023. Alzheimer's disease: A brief history of immunotherapies targeting amyloid β. Int. J. Mol. Sci. 24 (4), 3895.
Wang, L., Liu, Y., Zeng, X., Cheng, H., Wang, Z., Wang, Q., 2020. Region-of-interest based sparse feature learning method for Alzheimer's disease identification. Comput. Methods Programs Biomed. 187, 1–10.
Wang, K., Theeke, L.A., Liao, C., Wang, N., Lu, Y., Xiao, D., Xu, C., Initiative, A.D.N., et al., 2023. Deep learning analysis of UPLC-MS/MS-based metabolomics data to predict Alzheimer's disease. J. Neurol. Sci. 453, 120812.
Yamashita, R., Nishio, M., Do, R.K.G., Togashi, K., 2018. Convolutional neural networks: an overview and application in radiology. Insights Imaging 9, 611–629.
Yang, Z., Liu, Z., 2020. The risk prediction of Alzheimer's disease based on the deep learning model of brain 18F-FDG positron emission tomography. Saudi J. Biol. Sci. 27 (2), 659–665.
Yu, Y., Si, X., Hu, C., Zhang, J., 2019. A review of recurrent neural networks: LSTM cells and network architectures. Neural Comput. 31 (7), 1235–1270.